

CTRL-Adapter: An Efficient and Versatile Framework for Adapting Diverse Controls to Any Diffusion Model

Han Lin* Jaemin Cho* Abhay Zala Mohit Bansal
 UNC Chapel Hill
 {hanlincs, jmincho, aszala, mbansal}@cs.unc.edu
<https://ctrl-adapter.github.io>

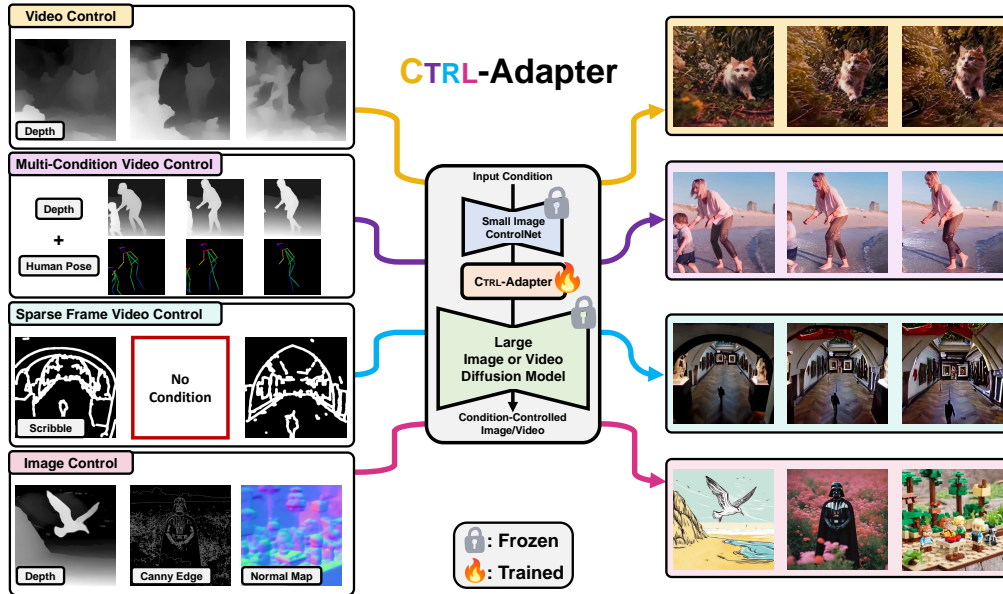


Figure 1: We propose **CTRL-Adapter**, an efficient and versatile framework for adding diverse spatial controls to any image or video diffusion model. CTRL-Adapter supports a variety of useful applications, including video control, video control with multiple conditions, video control with sparse frame conditions, image control, zero-shot transfer to unseen conditions, and video editing.

Abstract

ControlNets are widely used for adding spatial control in image generation with different conditions, such as depth maps, canny edges, and human poses. However, there are several challenges when leveraging the pretrained image ControlNets for controlled video generation. First, pretrained ControlNet cannot be directly plugged into new backbone models due to the mismatch of feature spaces, and the cost of training ControlNets for new backbones is a big burden for many users. Second, ControlNet features for different frames might not effectively handle the temporal consistency of objects. To address these challenges, we introduce **CTRL-Adapter**, an efficient and versatile framework that adds diverse controls to any image/video diffusion models, by adapting pretrained ControlNets (and improving temporal alignment for videos). CTRL-Adapter provides strong and diverse capabilities including image control, video control, video control with sparse frames, multi-condition control, compatibility with different backbone models, adaptation to unseen control conditions, and video editing. In the CTRL-Adapter framework, we train adapter layers that fuse pretrained ControlNet features

*equal contribution

to different image/video diffusion models, while keeping the parameters of the ControlNets and the diffusion models frozen. CTRL-Adapter consists of temporal as well as spatial modules so that it can effectively handle the temporal consistency of videos. Additionally, for robust adaptation to different backbone models and sparse control, we propose latent skipping and inverse timestep sampling. Moreover, CTRL-Adapter enables control from multiple conditions by simply taking the (weighted) average of ControlNet outputs. From our experiments with diverse image and video diffusion backbones (SDXL, Hotshot-XL, I2VGen-XL, and SVD), CTRL-Adapter matches ControlNet on the COCO dataset for image control, and even outperforms all baselines for video control (achieving the state-of-the-art accuracy on the DAVIS 2017 dataset) with significantly lower computational costs (CTRL-Adapter outperforms baselines in less than 10 GPU hours). Lastly, we provide comprehensive ablations for our design choices and qualitative examples.

1 Introduction

Recent diffusion models have achieved significant progress in generating high-fidelity images [52, 44, 56, 47] and videos [3, 15, 6, 35, 37] from text descriptions. As it is often hard to describe every image/video detail only with text, there have been many works to control diffusion models in a more fine-grained manner by providing additional condition inputs such as bounding boxes [33, 71], reference object images [54, 14, 31], and segmentation maps [13, 2, 74]. Among them, Zhang *et al.* [74] have released a variety of ControlNet checkpoints based on Stable Diffusion [52] v1.5 (SDv1.5), and the user community has also shared many ControlNets trained with different input conditions. This has made ControlNet [74] one of the most popular spatial control methods for image generation.

However, there are challenges when using the existing pretrained image ControlNets for controllable video generation. First, pretrained ControlNet cannot be directly plugged into new backbone models, and the cost for training ControlNets for new backbone models is a big burden for many users due to high computational costs. For example, training a ControlNet for SDv1.5 takes 500-600 A100 GPU hours.² Second, ControlNet is designed for controllable image generation; hence applying these pretrained ControlNets with image backbones directly to each video frame independently does not take the temporal consistency across video frames into account. This leads to an interesting question: *Can we design an efficient and versatile framework that can reuse and adapt any existing pretrained ControlNet to accurately guide new image/video diffusion models and support diverse controls?*

To address this challenge, we design **CTRL-Adapter**, a novel, flexible framework that enables the efficient reuse of pretrained ControlNets for diverse controls with any new image/video diffusion models, by adapting pretrained ControlNets (and improving temporal alignment for videos). We illustrate the overall capabilities of CTRL-Adapter framework in Fig. 1. As shown in Fig. 2 left, CTRL-Adapter trains adapter layers [26, 72] to map the features of a pretrained image ControlNet to a target image/video diffusion model, while keeping the parameters of the ControlNet and the backbone diffusion model frozen. As shown in Fig. 2 right, each CTRL-Adapter consists of four modules: spatial convolution, temporal convolution, spatial attention, and temporal attention. The temporal convolution/attention modules effectively fuse the ControlNet features into image/video diffusion models for better temporal consistency. Additionally, to ensure robust adaptation of ControlNets to backbone models of different noise scales and sparse frame control conditions, we propose skipping the visual latent variable from the ControlNet inputs. We also introduce inverse timestep sampling to effectively adapt ControlNets to new backbones equipped with continuous diffusion timestep samplers. For more accurate control beyond a single condition, CTRL-Adapter’s reuse of pretrained ControlNets also allows easy combination of multiple conditions (*e.g.*, using both depth map and canny edge as conditions) by simply taking the (weighted) average of different ControlNet outputs.

As shown in Table 1, CTRL-Adapter allows many useful capabilities including image control, video control, video control with sparse frames, multi-condition control, and compatibility with different backbone models, while previous methods only support a small subset of them (see details in Sec. 2). We demonstrate the effectiveness of CTRL-Adapter through extensive experiments and analyses. It

²<https://huggingface.co/lillyasviel/sd-controlnet-depth> and <https://huggingface.co/lillyasviel/sd-controlnet-canny>

Table 1: Overview of the capabilities supported by recent methods for controlled image/video generation. CTRL-Adapter supports five useful features, while previous methods support only some of them.

Method	Image Control	Video Control	Video Control w/ Sparse Frames	Multi-Condition Control	Compatible w/ Different Backbones
Image Control Methods					
ControlNet [74]	✓	✗	✗	✗	✗
Multi-ControlNet [74]	✓	✗	✗	✓	✗
T2I-Adapter [40]	✓	✗	✗	✓	✗
GLIGEN [33]	✓	✗	✗	✓	✗
Uni-ControlNet [78]	✓	✗	✗	✓	✗
UniControl [46]	✓	✗	✗	✓	✗
X-Adapter [48]	✓	✗	✗	✗	✓
Video Control Methods					
VideoComposer [66]	✗	✓	✗	✓	✗
AnimateDiff [18]+SparseCtrl [17]	✗	✓	✓	✗	✗
CTRL-Adapter (Ours)	✓	✓	✓	✓	✓

exhibits strong performance when adapting ControlNets (pretrained with SDv1.5) to various video and image diffusion backbones, including text-to-video generation (Hotshot-XL [41]), image-to-video generation (I2VGen-XL [75] and Stable Video Diffusion [3]), and text-to-image generation (SDXL [44]).

In our experiments, we first demonstrate that CTRL-Adapter matches the performance of a pretrained image ControlNet on COCO dataset [36] and outperforms previous methods in controllable video generation (achieving state-of-the-art performance on the DAVIS 2017 dataset [45]) with significantly lower computational costs (CTRL-Adapter outperforms baselines in less than 10 GPU hours). Next, we demonstrate that CTRL-Adapter enables more accurate video generation with multiple conditions compared to a single condition. Averaging ControlNet features with learnable linear weights enhances performance beyond that achieved by averaging with equal weights. In addition, we show that skipping the visual latent variable from ControlNet inputs allows video control only with a few frames of (*i.e.*, sparse) conditions, eliminating the need for dense conditions across all frames. We also highlight zero-shot adaption – CTRL-Adapter trained with one condition (*e.g.*, depth maps) can easily adapt to another ControlNet trained with a different condition (*e.g.*, segmentation maps). Lastly, we provide comprehensive ablations for CTRL-Adapter design choices and qualitative examples.

2 Related Works

Text-to-video and image-to-video generation models. Generating videos from text descriptions or images (*e.g.*, initial video frames) based on deep learning and has increasingly gained much attention. Early works for this task [34, 32, 77, 60] have commonly used variational autoencoders (VAEs) [30] and generative adversarial networks (GANs) [16], while most of recent video generation works are based on denoising diffusion models [24, 61]. Powered by large-scale training, recent video diffusion models demonstrate impressive performance in generating highly realistic videos from text descriptions [21, 23, 59, 79, 28, 63, 73, 64, 41, 42, 19, 39] or initial video frames (*i.e.*, images) [3, 75, 18, 70].

Adding control to image/video diffusion models. While recent image/video diffusion models demonstrate impressive performance in generating highly realistic images/videos from text descriptions, it is hard to describe every detail of images/videos only with text or first frame image. Instead, there have been many works using different types of additional inputs to control the image/video diffusion models, such as bounding boxes [33, 71], reference object image [54, 14, 31], segmentation map [13, 2, 74], sketch [74], *etc.*, and combinations of multiple conditions [29, 46, 78, 66]. As finetuning all the parameters of such image/video diffusion models is computationally expensive, several methods, such as ControlNet [74], have been proposed to add conditional control capability via parameter-efficient training [74, 55, 40]. X-Adapter [48] learns an adapter module to reuse ControlNets pretrained with a smaller image diffusion model (*e.g.*, SDv1.5) for a bigger image diffusion model (*e.g.*, SDXL). While they focus solely on learning an adapter for image control, CTRL-Adapter features architectural designs (*e.g.*, temporal convolution/attention layers) for video generation as well. In addition, X-Adapter needs the smaller image diffusion model (SDv1.5) during

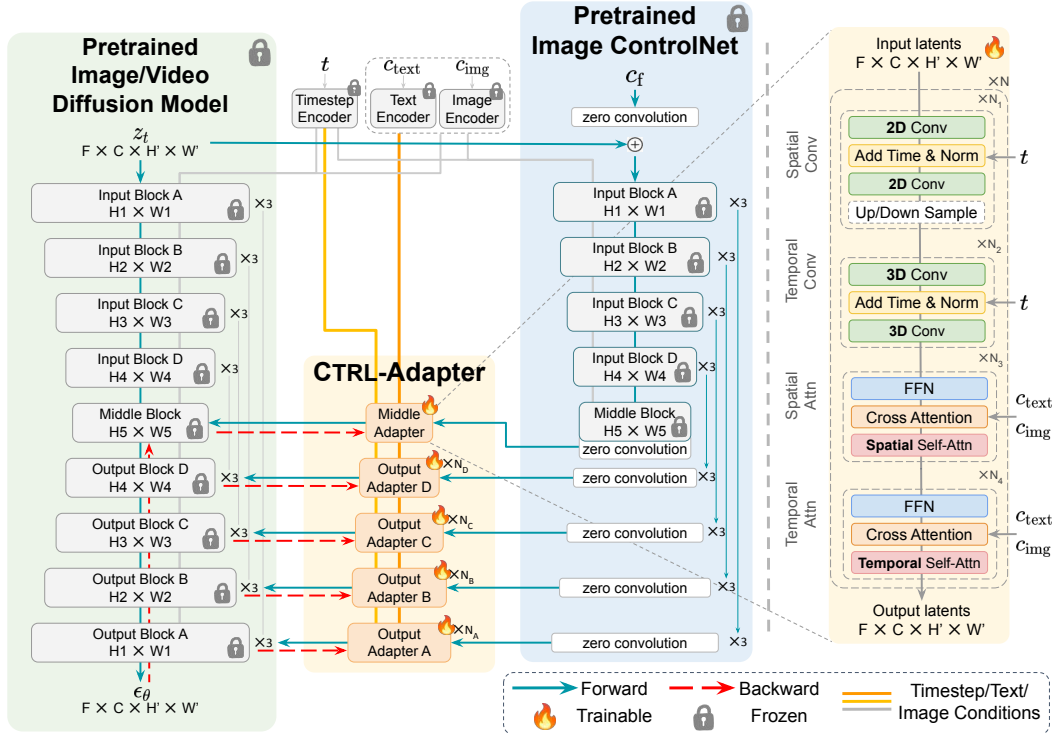


Figure 2: **Left:** CTRL-Adapter (colored orange) enables to reuse pretrained image ControlNets (colored blue) for new image/video diffusion models (colored green). **Right:** Architecture details of CTRL-Adapter. Temporal convolution and attention layers are skipped for image diffusion backbones.

training and inference, whereas CTRL-Adapter doesn't need the smaller diffusion model at all (for image/video generation), hence being more memory and computationally efficient (see Appendix C for details). SparseCtrl [17] guides a video diffusion model with conditional inputs of few frames (instead of full frames), to alleviate the cost of collecting video conditions. Since SparseCtrl involves augmenting ControlNet with an additional channel for frame masks, it requires training a new variant of ControlNet from scratch. In contrast, we leverage existing image ControlNets more efficiently by propagating information through temporal layers in adapters and enabling sparse frame control via skipping the latents from ControlNet inputs (see Sec. 3.2 for details). Furthermore, compared with previous works that are specially designed for specific condition controls on a single modality (image [74, 46] or video [27, 76]), our work presents a unified and versatile framework that supports diverse controls, including image control, video control, sparse frame control, and multi-source control, with significantly lower computational costs by reusing pretrained ControlNets (e.g., CTRL-Adapter outperforms baselines in less than 10 GPU hours). Table 1 summarizes the comparison of CTRL-Adapter with related works.

3 Method

In the section, we first explain the background of latent diffusion models and ControlNets (Sec. 3.1). Next, we introduce **CTRL-Adapter**, a novel framework that enables the efficient reuse of pretrained ControlNets for diverse controls with any new image/video diffusion models (Sec. 3.2). Our CTRL-Adapter matches or outperforms existing image/video control methods in both full-frame and sparse-frame condition settings, achieving state-of-the-art video control performance, with significantly lower training costs (e.g., CTRL-Adapter trained for 22 hours can match SDXL ControlNet trained for 700 hours; see Fig. 13). Lastly, we explain image/video generation with multiple conditions (e.g., depth/human pose) can be achieved by combining multiple ControlNets with different input conditions via a simple (weighted) averaging (Sec. 3.3).

3.1 Preliminaries: Latent Diffusion Models and ControlNets

Latent Diffusion Models. Many recent video generation works are based on latent diffusion models (LDMs) [52], where a diffusion model learns the temporal dynamics of compact latent representations of videos. First, given a F -frame RGB video $\mathbf{x} \in \mathbb{R}^{F \times 3 \times H \times W}$, a video encoder (of a pretrained autoencoder) provides C -dimensional latent representation (*i.e.*, latents): $\mathbf{z} = \mathcal{E}(\mathbf{x}) \in \mathbb{R}^{F \times C \times H' \times W'}$, where height and width are spatially downsampled ($H' < H$ and $W' < W$). Next, in the forward process, a noise scheduler such as DDPM [24] gradually adds noise to the latents \mathbf{z} : $q(\mathbf{z}_t | \mathbf{z}_{t-1}) = N(\mathbf{z}_t; \sqrt{1 - \beta_t} \mathbf{z}_{t-1}, \beta_t \mathbf{I})$, where $\beta_t \in (0, 1)$ is the variance schedule with $t \in \{1, \dots, T\}$. Then, in the backward pass, a diffusion model (usually a U-Net architecture) $\mathcal{F}_\theta(\mathbf{z}_t, t, \mathbf{c}_{\text{text/img}})$ learns to gradually denoise the latents, given a diffusion timestep t , and a text prompt \mathbf{c}_{text} (*i.e.*, T2V) or an initial frame \mathbf{c}_{img} (*i.e.*, I2V) if provided. The diffusion model is trained with following objective: $\mathcal{L}_{\text{LDM}} = \mathbb{E}_{\mathbf{z}, \epsilon \sim N(0, \mathbf{I}), t} \|\epsilon - \epsilon_\theta(\mathbf{z}_t, t, \mathbf{c}_{\text{text/img}})\|_2^2$, where ϵ and ϵ_θ represent the added noise to latents and the predicted noise by \mathcal{F}_θ respectively. We apply the same objective for CTRL-Adapter training.

ControlNets. ControlNet [74] is designed to add spatial controls to image diffusion models in the form of different guidance images (*e.g.*, depth, sketch, segmentation maps, *etc.*). Specifically, given a pretrained backbone image diffusion model \mathcal{F}_θ that consists of input/middle/output blocks, ControlNet has a similar architecture $\mathcal{F}_{\theta'}$, where the input/middle blocks parameters of θ' are initialized from θ , and the output blocks consist of 1x1 convolution layers initialized with zeros. ControlNet takes the diffusion timestep t , text prompt \mathbf{c}_{text} , and control images \mathbf{c}_f (*e.g.*, depth image for each frame) as inputs, and provides the features that are merged into output blocks of backbone image model ϵ_θ to generate the final image. The authors of ControlNet have released a variety of ControlNet checkpoints based on Stable Diffusion [52] v1.5 (SDv1.5) and the user community have also shared many ControlNets trained with different input conditions based on SDv1.5. However, these ControlNets cannot be used with more recently released bigger and stronger image/video diffusion models, such as SDXL [44] and I2VGen-XL [75]. Moreover, the input/middle blocks of the ControlNet are in the same size with those of the diffusion backbones (*i.e.*, if the backbone model gets bigger, ControlNet also gets bigger). Due to this, it becomes increasingly difficult to train new ControlNets for each bigger and newer model that is released over time. To address this, we introduce CTRL-Adapter for efficient adaption of existing ControlNets for new diffusion models.

3.2 CTRL-Adapter

We introduce **CTRL-Adapter**, a novel framework that enables the efficient reuse of existing image ControlNets (of SDv1.5) for spatial control with new diffusion models. *We mainly describe our method details in the video generation settings, since CTRL-Adapter can be flexibly adapted to image diffusion models by regarding images as single-frame videos.*

Efficient Adaptation of Pretrained ControlNets. As shown in Fig. 2 (left), we train an adapter module (colored orange) to map the middle/output blocks of a pretrained ControlNet (colored blue) to the corresponding middle/output blocks of the target video diffusion model (colored green). If the target backbone does not have the same number of output blocks CTRL-Adapter maps the ControlNet features to the output block that handles the closest height and width of the latents. We keep all parameters in both the ControlNet and the target video diffusion model frozen. Therefore, training a CTRL-Adapter can be significantly more efficient than training a new video ControlNet.

CTRL-Adapter architecture. As shown in Fig. 2 (right), each block of CTRL-Adapter consists of four modules: spatial convolution, temporal convolution, spatial attention, and temporal attention. We set the values for $N_{1:4}$ and N as 1 by default. All four modules aim to align the image ControlNet features with those of target video diffusion models. And the temporal convolution and attention modules model effectively fuse the in ControlNet features for better temporal consistency. Moreover, the spatial/temporal convolution modules incorporate the current denoising timestep t and spatial/temporal convolution modules incorporate the conditions (*i.e.*, text prompt/initial frame) $\mathbf{c}_{\text{text/img}}$. This design allows the CTRL-Adapter to dynamically adjust its features according to different denoising stages and the objects generated. When adapting to image diffusion models, CTRL-Adapter blocks only consist of spatial convolution/attention modules (without temporal convolution/attention

modules). See Section 6.1 for detailed ablation studies on the design choices of CTRL-Adapter, and see Appendix B for the implementation details of the four modules.

Skipping the latent from ControlNet inputs: robust adaption to different noise scales & sparse frame conditions.

Although the original ControlNets take the latent z_t as part of their inputs, we find that skipping z_t from ControlNet inputs is effective for CTRL-Adapter in certain settings, as illustrated in Fig. 3. **(1) Different noise scales:** while SDv1.5 samples noise ϵ from $N(0, I)$, some recent diffusion models [25, 10, 3] sample noise ϵ of much bigger scale (e.g. SVD [3] sample noise from $\sigma * N(0, I)$, where $\sigma \sim \text{LogNormal}(0.7, 1.6)$; $\sigma \in [0, +\infty]$ and $\mathbb{E}[\sigma] = 7.24$). We find that adding larger-scale z_t from the new backbone models to image conditions c_f dilutes the c_f and makes the ControlNet outputs uninformative, whereas skipping z_t enables the adaptation of such new backbone models. **(2) Sparse frame conditions:** when the image conditions are provided only for the subset of video frames (i.e., $c_f = \emptyset$ for most frames f), ControlNet could rely on the information from z_t and ignore c_f during training. Skipping z_t from ControlNet inputs also helps the CTRL-Adapter to more effectively handle such sparse frame conditions (see Table 5).

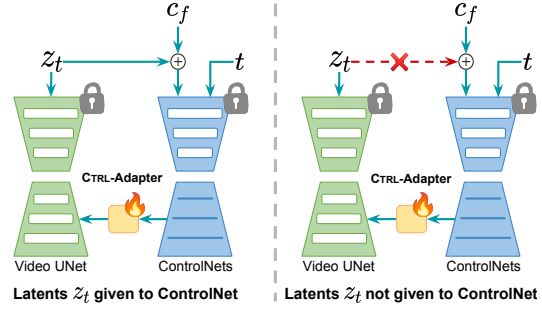


Figure 3: **Left:** latent z_t is given to ControlNets (default CTRL-Adapter). **Right:** latent z_t is not given to ControlNet.

Inverse timestep sampling: robust adaptation to continuous diffusion timestep samplers.

While SDv1.5 samples discrete timesteps t uniformly from $\{0, 1, \dots, 1000\}$, some recent diffusion models [10, 38, 51] sample timesteps from continuous distributions, e.g., SVD [3] first samples noise scale σ_{SVD} from a log-normal distribution $\sigma_{\text{SVD}} \sim \text{LogNormal}(0.7, 1.6)$, and then sets the timestep t_{SVD} as a function of σ_{SVD} : $t_{\text{SVD}} = 0.25 \log \sigma_{\text{SVD}}$. This gap between discrete and continuous distributions means that we cannot assign the same timestep t to both the video diffusion model and the ControlNet. Therefore, we propose **inverse timestep sampling**, an algorithm that creates a mapping between the continuous and discrete time distributions to match different timestep samplers (see Algorithm 1 for PyTorch [1] code). During each training step, the procedure for this algorithm can be summarized as follows: **(1)** we sample a variable u from Uniform[0, 1]; **(2)** we sample noise scale σ_{cont} via inverse transform sampling; i.e., we derive the inverse cumulative density function of σ_{cont} and sample σ_{cont} by sampling u : $\sigma_{\text{cont}} = F_{\text{cont}}^{-1}(u)$; **(3)** given a preconditioning function g_{cont} that maps noise scale to timestep (typically associated with the continuous-time noise sampler), we can compute $t_{\text{cont}} = g_{\text{cont}}(\sigma_{\text{cont}})$; **(4)** we set the timesteps and noise scales for both ControlNet and our CTRL-Adapter as $t_{\text{CNet}} = 1000u$ and $\sigma_{\text{CNet}} = u$ respectively, where 1000 represents the denoising timestep range over which the ControlNet is trained. During inference, we uniformly sample k equidistant values for u within [0, 1] and derive corresponding $t_{\text{cont./CNet}}$ and $\sigma_{\text{cont./CNet}}$ as inputs for denoising steps.

3.3 Multi-Condition Generation via CTRL-Adapter Composition

For more effective spatial control beyond a single condition, we can easily combine the control features of multiple ControlNets via our CTRL-Adapter. As shown in Fig. 4, we first average the ControlNet output features via learnable scalar weights (i.e., $w_1, w_2, \dots, w_N, \sum_{i=1}^N w_i = 1$), for each CTRL-Adapter block, then provide such fused ControlNet features as input to a shared and unified CTRL-Adapter. The weighted-average approach can be understood as a lightweight mixture-of-experts (MoE) [58]. For training the weights, we first randomly select an integer k from the set $\{1, 2, \dots, N_{\text{max}}\}$, where N_{max} is a hyper-parameter that balances

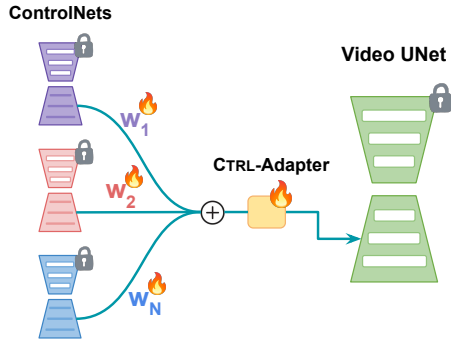


Figure 4: Multi-condition video generation by combining multiple ControlNets.

training speed and composition (default as 4 in our experiments). Then we randomly choose k ControlNets and average the outputs of the selected ControlNet with the learned weights.

4 Experimental Setup

4.1 ControlNets and Target Diffusion Models

ControlNets. We use ControlNets trained with SDv1.5.³ SDv1.5 has the most number of publicly released ControlNets and has a much smaller training cost compared to recent image/video diffusion models. Note that unlike X-Adapter [48], CTRL-Adapter does not need to load the source diffusion model (SDv1.5) during training or inference (see (a) and (d) in Fig. 17 for model architecture comparison).

Target diffusion models (where ControlNets are to be adapted). For video generation models, we experiment with one text-to-video generation model – Hotshot-XL [41], and two image-to-video generation models – I2VGen-XL [75] and Stable Video Diffusion (SVD) [3]. For image generation model, we experiment with the base model in SDXL [44]. For all models, we use their default settings during training and inference (*e.g.*, number of output frames, resolution, number of denoising steps, classifier-free guidance scale, *etc.*).

4.2 Training Datasets for CTRL-Adapter

Video datasets. For training CTRL-Adapter for video diffusion models, we use 0.2M videos randomly sampled from the Panda-70M training set [7]. Following recent works [3, 9], we filter out videos of static scenes by removing videos whose average optical flow [11, 4] magnitude is below a certain threshold. Concretely, we use the Gunnar Farneback’s algorithm⁴ [12] at 2FPS, calculate the averaged the optical flow for each video and re-scale it between 0 and 1, and filter out videos whose average optical flow error is below a threshold of 0.25. This process gives us a total of 0.2M remaining videos.

Image datasets. For training CTRL-Adapter for image diffusion models, we use 300K images randomly sampled from LAION POP,⁵ which is a subset of LAION 5B [57] dataset and contains 600K images in total with aesthetic values of at least 0.5 and a minimum resolution of 768 pixels on the shortest side. As suggested by the authors, we use the image captions generated with CogVLM [65].

4.3 Input Conditions

We extract various input conditions from the video and image datasets described above.

- **Depth map:** As recommended in Midas⁶ [49], we employ `dpt_swin2_large_384` for the best speed-performance trade-off.
- **Canny edge, surface normal, line art, softedge, and user sketching/scribbles:** Following ControlNet [74], we utilize the same annotator implemented in the `controlnet_aux`⁷ library.
- **Semantic segmentation map:** To obtain higher-quality segmentation maps than UPerNet [68] used in ControlNet, we employ SegFormer [69] `segformer-b5-finetuned-ade-640-640` finetuned on ADE20k dataset at 640×640 resolution.
- **Human pose:** We employ ViTPose [69] `ViTPose_huge_simple_coco` to improve both processing speed and estimation quality, compared to OpenPose [5] used in ControlNet.

³<https://huggingface.co/llyasviel/ControlNet>

⁴https://docs.opencv.org/4.x/d4/dee/tutorial_optical_flow.html

⁵<https://laion.ai/blog/laion-pop/>

⁶<https://github.com/is1-org/MiDaS>

⁷https://github.com/huggingface/controlnet_aux

Table 2: Evaluation of video generation with single control condition (depth map/canny edge) on DAVIS 2017 dataset. †: skipping latents z to ControlNet input to handle different noise scale (see Sec. 3.2 for details).

Method	Depth Map		Canny Edge	
	FID (\downarrow)	Optical Flow Error (\downarrow)	FID (\downarrow)	Optical Flow Error (\downarrow)
Text2Video-Zero [28]	19.46	4.09	17.80	3.77
ControlVideo [76]	27.84	4.03	25.58	3.73
Control-A-Video [8]	22.16	3.61	22.82	3.44
VideoComposer [66]	22.09	4.55	-	-
Hotshot-XL backbone				
SDXL ControlNet [62]	45.35	4.21	25.40	4.43
SDv1.5 ControlNet + CTRL-Adapter (Ours)	14.63	3.94	20.83	4.15
I2VGen-XL backbone				
SDv1.5 ControlNet + CTRL-Adapter (Ours)	7.43	3.20	6.42	3.37
SVD backbone				
SVD Temporal ControlNet [53]	4.91	4.84	-	-
SDv1.5 ControlNet + CTRL-Adapter† (Ours)	4.05	3.68	4.16	3.96

4.4 Evaluation datasets

Video datasets. Following previous works [27, 76], we evaluate our video ControlNet adapters on DAVIS 2017 [45], a public benchmark dataset also used in other controllable video generation works [27]. We first combine all video sequences from TrainVal, Test-Dev 2017 and Test-Challenge 2017. Then, we chunk each video into smaller clips, with the number of frames in each clip being the same as the default number of frames generated by each video backbone (*e.g.*, 8 frames for Hotshot-XL, 16 frames for I2VGen-XL, and 14 frames for SVD). This process results in a total of 1281 video clips of 8 frames, 697 clips of 14 frames, and 608 video clips of 16 frames.

Image datasets. We evaluate our image ControlNet adapters on COCO val2017 split [36], which contains 5k images that cover diverse range of daily objects. We resize and center crop the images to 1024 by 1024 for SDXL evaluation.

4.5 Evaluation Metrics

Visual quality. Following previous works [46, 27], we use Frechet Inception Distance (FID) [22] to measure the distribution distance between our generated images/videos and input images/videos.⁸

Spatial control. For video datasets, following VideoControlNet [27], we report the L2 distance between the optical flow [50] of the input video and the generated video (Optical Flow Error). For image datasets, following Uni-ControlNet [78], we report the Structural Similarity (SSIM) [67]⁹ and mean squared error (MSE)¹⁰ between generated images and ground truth images.

5 Results and Analysis

We demonstrate the usefulness of CTRL-Adapter with comprehensive experiments and analysis. We first evaluate CTRL-Adapter for controlled video (Sec. 5.1) and image generation (Sec. 5.2). Then we evaluate the combination of multiple CTRL-Adapter for video generation with multiple conditions (Sec. 5.3). We also experiment video generation with sparse frame conditions (Sec. 5.4) and zero-shot generalization on unseen conditioned modalities (Sec. 5.5). Moreover, we analyze the training efficiency of CTRL-Adapter (Sec. 5.6). Lastly, we showcase a video editing pipeline by controlling both image and video diffusion models with CTRL-Adapter (Sec. 5.7).

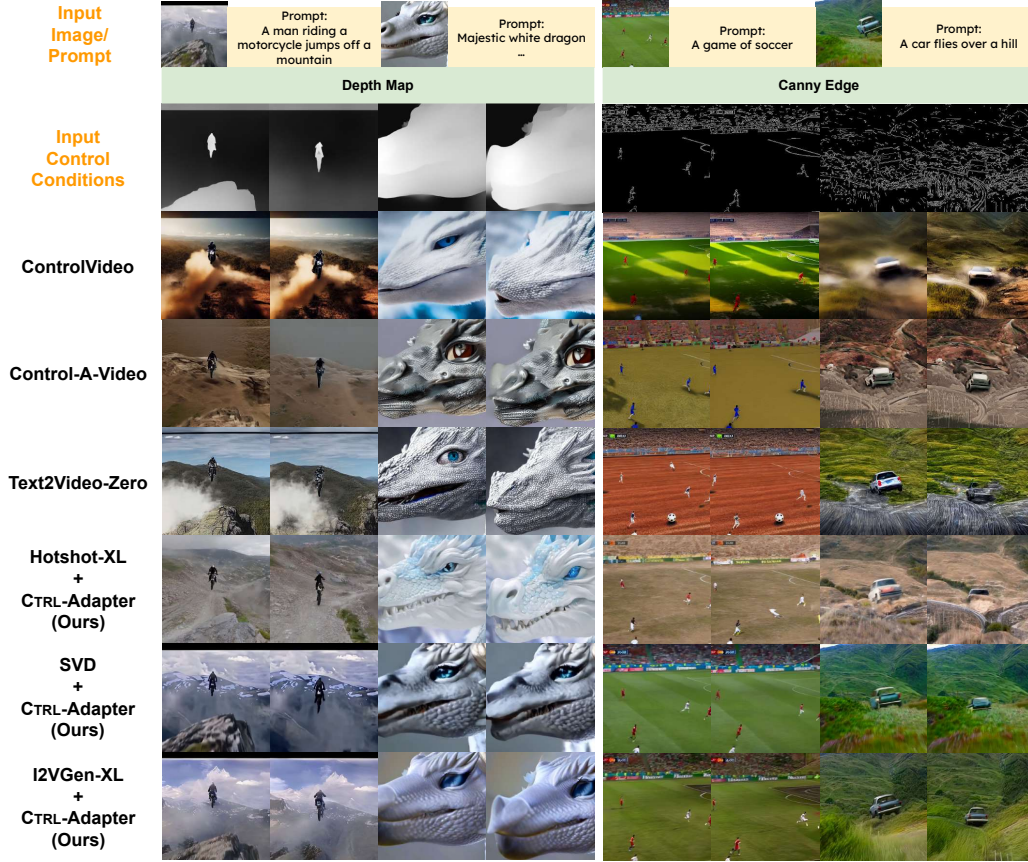


Figure 5: Video generation with different video control methods and CTRL-Adapter using depth map (left) and canny edge (right) conditions. See full videos on our project page.

5.1 Video Generation with Single Control Condition

We experiment with CTRL-Adapter on a text-to-video (T2V) generation backbone, Hotshot-XL [41], and two image-to-video (I2V) generation backbones, I2VGen-XL [75] and Stable Video Diffusion (SVD) [3]. We compare our method with previous controllable video generation models, including Text2Video-Zero [28], Control-A-Video [8], ControlVideo [76], and VideoComposer [66]. As the spatial layers of Hotshot-XL are initialized with SDXL and remain frozen, the SDXL ControlNets are directly compatible with Hotshot-XL, so we include Hotshot-XL + SDXL ControlNet as a baseline. We also experiment with a temporal ControlNet [53] trained with SVD. While previous works (ControlVideo, Control-A-Video, Text2Video-Zero) generate 8-frame videos, CTRL-Adapter can flexibly adapt ControlNets to different video backbones that output equal length or even longer videos: Hotshot-XL (8 frames), SVD (14 frames) and I2VGen-XL (16 frames). Following Hu *et al.* [27], we evaluate all methods with FID and optical flow error.

SDv1.5 ControlNet + CTRL-Adapter outperforms other video control methods. Table 2 shows that in both depth map and canny edge input conditions, CTRL-Adapters on I2VGen-XL and SVD outperforms all previous strong video control methods in visual quality (FID) and spatial control (optical flow error) metrics. Note that it takes less than 10 GPU hours for CTRL-Adapter to outperform the baselines (see Sec. 5.6). In Fig. 5, we compare CTRL-Adapter and other recent video control

⁸To be consistent with the numbers reported in Uni-ControlNet [78], we use pytorch-fid (<https://github.com/mseitzer/pytorch-fid>) in Table 3. For other results, we use clean-fid [43] (<https://github.com/GaParmar/clean-fid>) which is more robust to aliasing artifacts.

⁹https://scikit-image.org/docs/stable/auto_examples/transform/plot_ssim.html

¹⁰<https://scikit-learn.org/stable/modules/classes.html#module-sklearn.metrics>



Figure 6: Videos generated from different video control methods and CTRL-Adapter on DAVIS 2017, using depth map (left) and canny edge (right) conditions. See full videos on our project page.

Table 3: Evaluation of image generation with single control condition (depth map/canny edge) on COCO val2017 split.

Method	Depth Map			Canny Edge	
	FID (↓)	MSE (↓)	SSIM (↑)	FID (↓)	SSIM (↑)
SDv1.4 or v1.5 backbone					
SDv1.5 ControlNet [74]	21.25	87.57	-	18.90	0.4828
T2I-Adapter [40]	21.35	89.82	-	18.98	0.4422
GLIGEN [33]	21.46	88.22	-	24.74	0.4226
Uni-ControlNet [78]	21.20	91.05	-	17.79	0.4911
SDXL backbone					
SDXL ControlNet [62]	17.91	86.95	0.8363	17.21	0.4458
SDv1.5 ControlNet + X-Adapter [48]	20.71	90.08	0.7885	19.71	0.3002
SDv1.5 ControlNet + CTRL-Adapter (Ours)	18.68	87.54	0.8515	21.77	0.5101

methods. When applied to three different backbones, CTRL-Adapter can handle challenging big/rapid movement controls. In Fig. 6, we also show videos generated on DAVIS 2017 dataset (described in Sec. 4.4).

5.2 Image Generation with Single Control Condition

We compare CTRL-Adapter with recent image control methods that use SDv1.4, SDv1.5 and SDXL as backbones. For methods using SDv1.4/v1.5 as a backbone, we compare CTRL-Adapter to pretrained SDv1.5 ControlNet [74], GLIGEN [33], T2I-Adapter [40], and Uni-ControlNet [78]. For methods

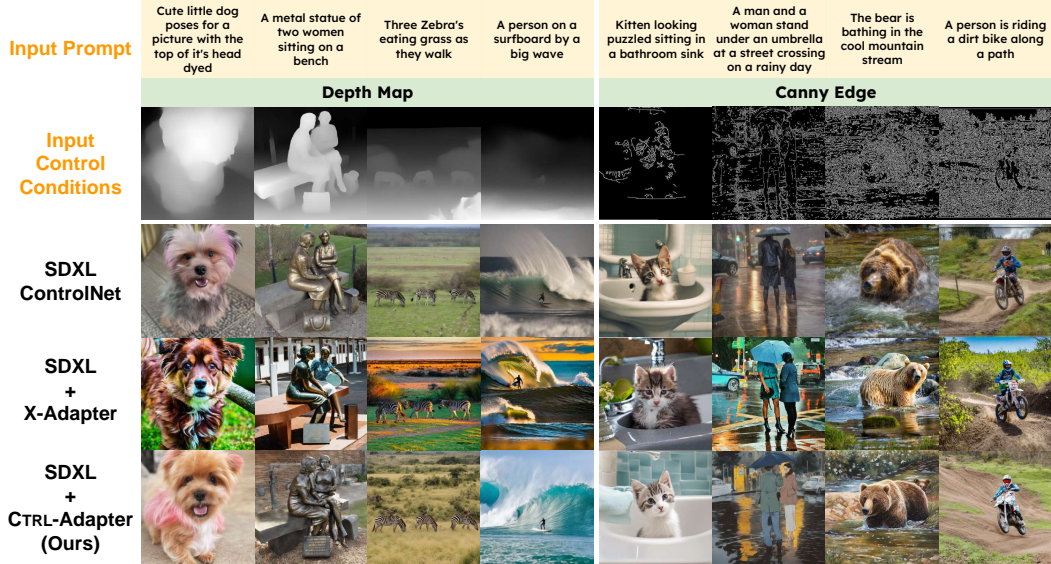


Figure 7: Image generation results on COCO val2017 split using depth map and canny edge conditions. CTRL-Adapter achieves better spatial control compared to X-Adapter (e.g., the arm of the metal statue for the second depth map input, the location of the person for the last depth map input, the tilt of the kitten’s head for the first canny edge input, and the bike’s orientation for the last canny edge input) and matches the performance of SDXL ControlNet.

using SDXL as a backbone, we compare CTRL-Adapter to pretrained SDXL ControlNet [62] and X-Adapter [48]. Following Zhao *et al.* [78], we report the FID, MSE, and SSIM scores.

SDv1.5 ControlNet + CTRL-Adapter outperforms other baselines and matches SDXL ControlNet. As shown in Table 3, we find that CTRL-Adapter outperforms all baselines with SDv1.4/v1.5 in most metrics (FID/MSE with depth map inputs and SSIM with canny edge inputs). When compared to the baselines with SDXL backbones, CTRL-Adapter outperforms X-Adapter in most metrics, and matches (in FID/MSE with depth map inputs) or outperforms SDXL ControlNet (in SSIM with depth map and canny edge inputs). Note that SDXL ControlNet was trained for much longer than CTRL-Adapter (700 vs. 22 A100 GPU hours) and it takes less than 10 GPU hours for CTRL-Adapter to outperform the SDXL ControlNet in SSIM in depth map (see Sec. 5.6). In Fig. 7, we show the image control methods with SDXL backbones. CTRL-Adapter achieves better spatial control compared to X-Adapter (e.g., the arm of the metal statue for the second depth map input, the location of the person for the last depth map input, the bear’s orientation for the third canny edge input, and the bike’s orientation for the last canny edge input) and matches the performance of SDXL ControlNet.

5.3 Video Generation with Multiple Control Conditions

As described in Sec. 3.3, users can easily achieve multi-source control by simply combining the control features of multiple ControlNets via our CTRL-Adapter. In Table 4, we compare the multi-source and single-source controlled video generation results with I2VGen-XL backbone in terms of visual quality (FID) and spatial control (optical flow error).

More conditions improve spatial control in video generation. Table 4 shows a clear trend that control with multiple conditions almost always yields better spatial control (lower optical flow error) and slightly lower visual quality (higher FID) than control with a single condition. See also Appendix D.2 for additional study on visual quality-spatial control tradeoff. Among different conditions, we find the combination of depth map and canny edges is more helpful than depth map and human pose, perhaps because not all videos include humans. Fig. 8 shows example videos generated with single and multiple conditions. While all videos correctly capture the high-level dynamics of ‘a woman wearing purple strolling during sunset’, the videos generated with more conditions show more robustness in several minor artifacts. For example, when only depth map is

Table 4: Comparison of single and multi-condition video generation with CTRL-Adapter. We adapt SDv1.5 ControlNets to I2VGen-XL and use DAVIS 2017 dataset for evaluation. The control sources are abbreviated as D (depth map), C (canny edge), N (surface normal), S (softedge), Seg (semantic segmentation map), L (line art), and P (human pose).

Conditions	FID (↓)	Optical Flow Error (↓)
Single condition		
D	7.43	3.20
C	6.42	3.37
Multiple conditions with equal weights		
D + C	8.50	2.84
D + P	11.32	3.48
D + C + N + S	8.75	2.40
D + C + N + S + Seg + L + P	9.48	2.93
Multiple conditions with linear weights (default)		
D + C	9.14	2.89
D + P	10.98	3.32
D + C + N + S	8.39	2.23
D + C + N + S + Seg + L + P	8.18	2.48

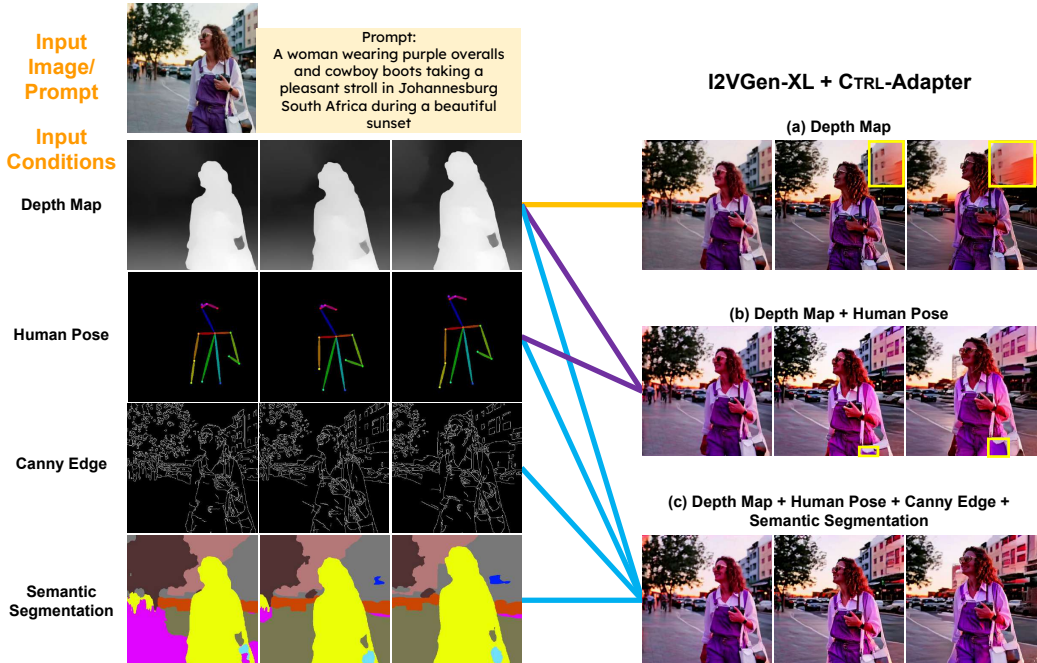


Figure 8: Video generation from single and multiple conditions with CTRL-Adapter on I2VGen-XL. (a) single condition: depth map; (b) 2 conditions: depth map + human pose; (c) 4 conditions: depth map + human pose + canny edge + semantic segmentation. While all videos correctly capture high-level dynamics, adding more conditions can help fix several minor artifacts (e.g., in (a) – building is blurred; in (b) – purse color changes).

given (Fig. 8 a), the building behind the person is blurred. When depth map and human pose are given (Fig. 8 b), the color of the purse changes from white to purple. When four conditions (depth map, canny edge, human pose, and semantic segmentation) are given, such artifacts are removed (Fig. 8 c). Fig. 9 shows additional generation examples with the four conditions (a woman with a child / a dancing man).

Linear weight is better than equal weights. When comparing equal weights and linear weights for averaging ControlNet features, Table 4 shows that in both FID and optical flow error, the linear weight outperforms the equal-weight approach as the number of conditions increases. This performance gain arises from the flexibility that allows various ControlNet experts to contribute differently in

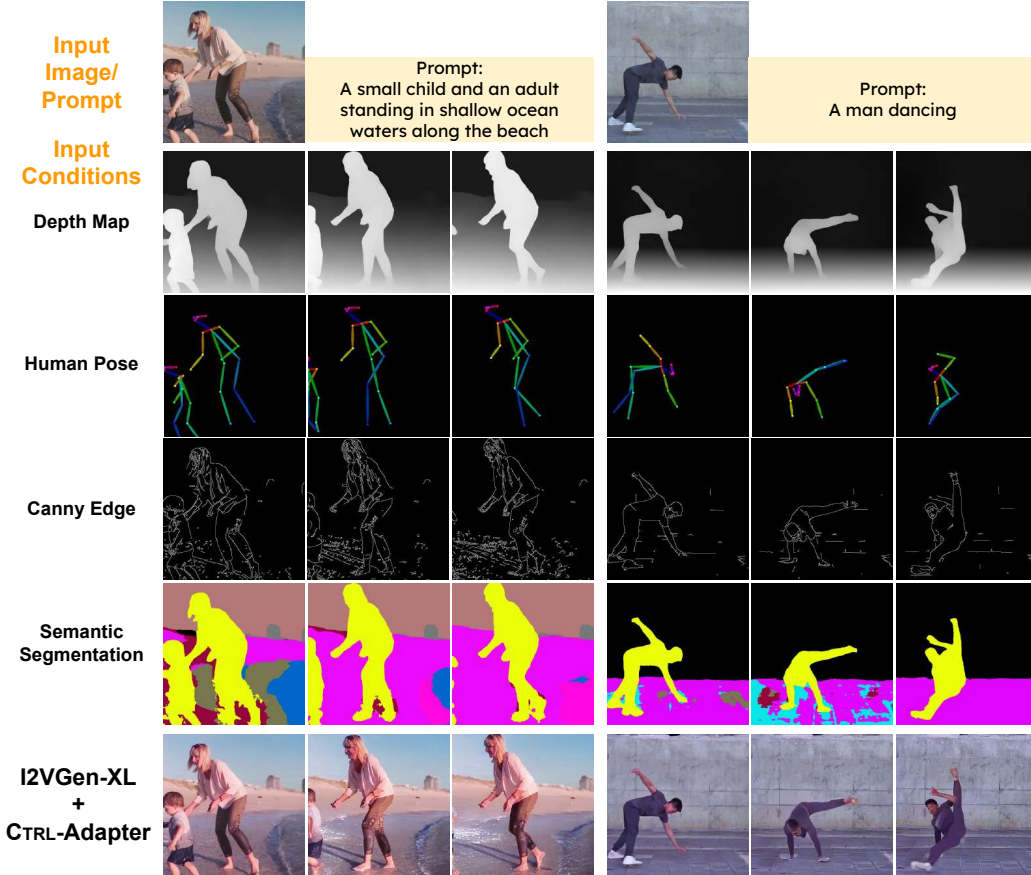


Figure 9: Additional video generation from 4 conditions: depth map + human pose + canny edge + semantic segmentation. See full videos on our project page.

each middle and output block. We visualize the learned weights for each control condition across all mid/output blocks in Fig. 25. In Table 6, we show additional experiments with learning a small MLP-based router module to assign weights to fuse ControlNet outputs, where the simple linear weights perform similarly.

5.4 Video Generation with Sparse Frames as Control Condition

We experiment CTRL-Adapter with providing sparse frame conditions (*i.e.*, conditions are given for only a subset of frames), using the I2VGen-XL backbone. During each training step, we first randomly select an integer $k \in \{1, \dots, N\}$, where N is equal to the total number of output frames of the video generation backbone (*e.g.*, $N = 16$ for I2VGen-XL). Next, we randomly select k keyframes from N total frames. We then extract these keyframes’ depth maps and user scribbles as control conditions. As explained in Sec. 3.2, we do not give the latents z and only give the k frames to ControlNet.

CTRL-Adapter can effectively handle sparse video control conditions. In Fig. 10, we can see that I2VGen-XL with our CTRL-Adapter can correctly generate videos that follow the scribble conditions for the given 4 sparse keyframes (out of a total of 16) and make reasonable interpolations on the frames without conditions. In Sec. 6.2, we also show that skipping the latent from ControlNet inputs is important in improving the sparse control capability.

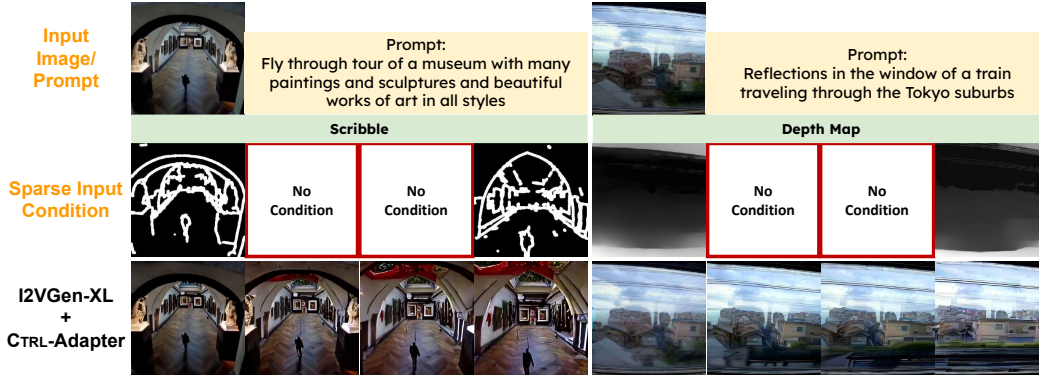


Figure 10: Video generation from sparse frame conditions with CTRL-Adapter on I2VGen-XL backbone. I2VGen-XL generates 16-frame videos, where we provide sparse control conditions (user scribble or depth map) for 1st, 6th, 11th, and 16th frames. See full videos on our project page.

5.5 Zero-Shot Generalization on Unseen Conditions

Since the majority of ControlNet parameters are the same as their backbone generation models, ControlNet can be interpreted as an image feature extractor that maps different types of images to the unified representation of backbone generation models. This begs an interesting question: “Does CTRL-Adapter learn general feature mapping from one (smaller) backbone to another (larger) backbone model?” To answer this question, we experiment with directly using CTRL-Adapter to adapt ControlNets that CTRL-Adapter have not seen during training. In Fig. 11, we show the CTRL-Adapter trained with a depth map SDv1.5 ControlNet can successfully adapt different SDv1.5 ControlNets that encode surface normal map, line art, and softedge conditions in a zero-shot manner.

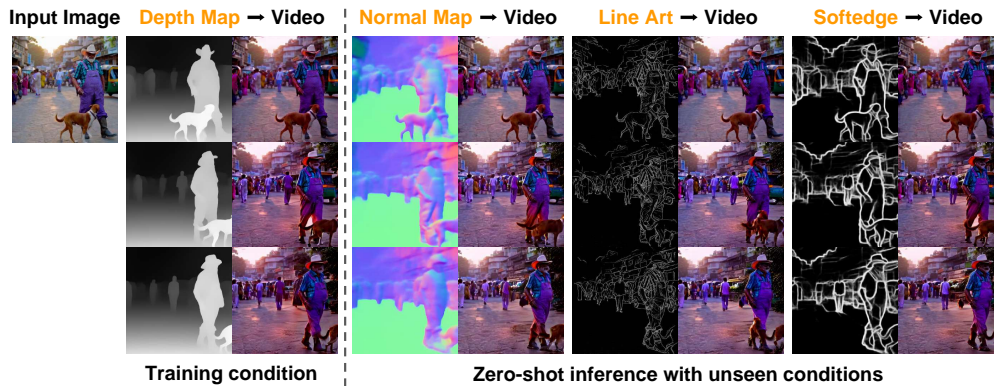


Figure 11: Zero-shot transfer of CTRL-Adapter trained only on depth maps to unseen conditions. See full videos on our project page.

5.6 Training Efficiency of CTRL-Adapter

In Fig. 12, we show generated images from CTRL-Adapter with different training hours. CTRL-Adapter learns to adapt the SDv1.5 ControlNet features to SDXL very quickly after a few hours, whereas training a ControlNet for SDXL takes 700 A100 hours. In Fig. 13, we show the training progress of CTRL-Adapter for video and image control. CTRL-Adapter outperforms strong baselines in less than 10 GPU hours.

5.7 Video Editing via Combining Image and Video CTRL-Adapters

In Fig. 14, we showcase that CTRL-Adapter can make video editing easy by cascading an image diffusion model (e.g., SDXL) and an image-to-video diffusion model (e.g., I2VGen-XL) where both

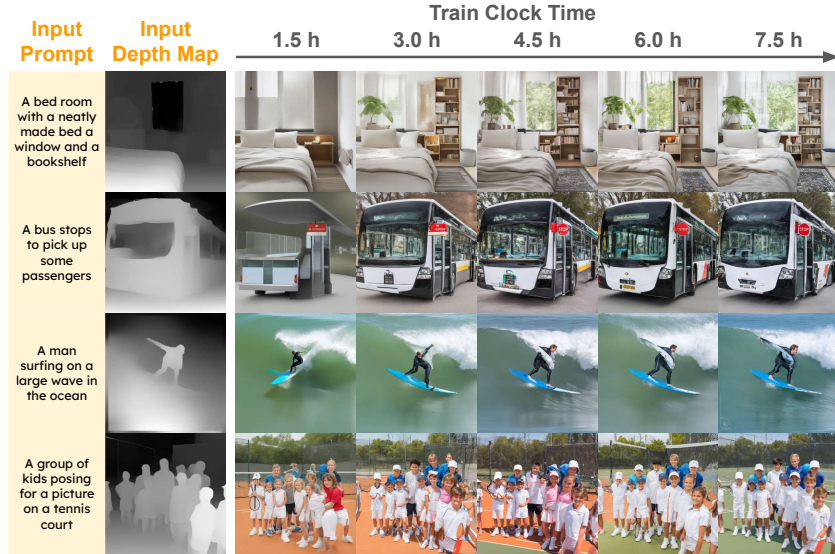


Figure 12: Training efficiency of CTRL-Adapter on SDXL backbone. Training clock time is measured on 4 A100 80GB GPUs.

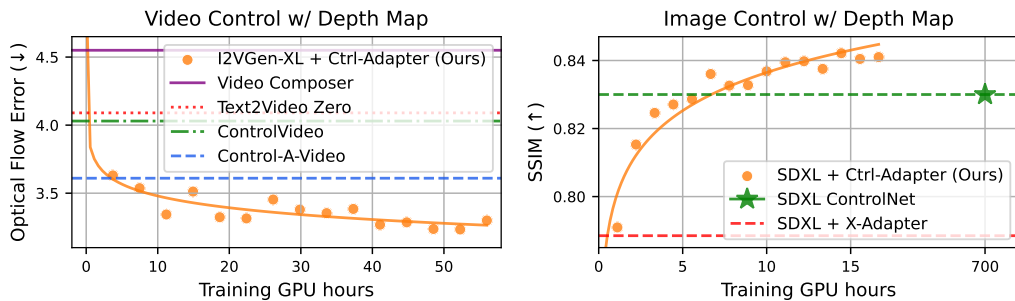


Figure 13: Training speed of CTRL-Adapter for video (left) and image (right) control with depth map. The training GPU hours are measured with A100 80GB GPUs. For both video and image controls, CTRL-Adapter outperforms strong baselines in less than 10 GPU hours.

models are equipped with spatial control via CTRL-Adapters. First, we extract conditions (*e.g.*, depth map) from the original video. Next, we create the initial frame with the image diffusion model (SDXL + CTRL-Adapter). Lastly, we provide the newly generated initial frame and frame-wise conditions to the image-to-video diffusion model (I2VGen-XL + CTRL-Adapter) to obtain the final edited video.

6 Ablation Studies

In the following, we show ablation studies for the design choices of CTRL-Adapter: different adapter architectures (Sec. 6.1) and skipping the latent to ControlNet inputs (Sec. 6.2).

6.1 Adapter Design

As described in Sec. 3.2, each CTRL-Adapter module consists of four components: spatial convolution (SC), temporal convolution (TC), spatial attention (SA), and temporal attention (TA). We experiment with different architecture combinations of the adapter components for image and video control, and plot the results in Fig. 15. Compared to X-Adapter [48], which uses a stack of three spatial convolution modules (*i.e.*, ResNet [20] blocks) for adapters, and VideoComposer [66], which employs spatial convolution + temporal attention for spatiotemporal condition encoder, we explore a richer combination that enhances global understanding of spatial information through spatial attention and

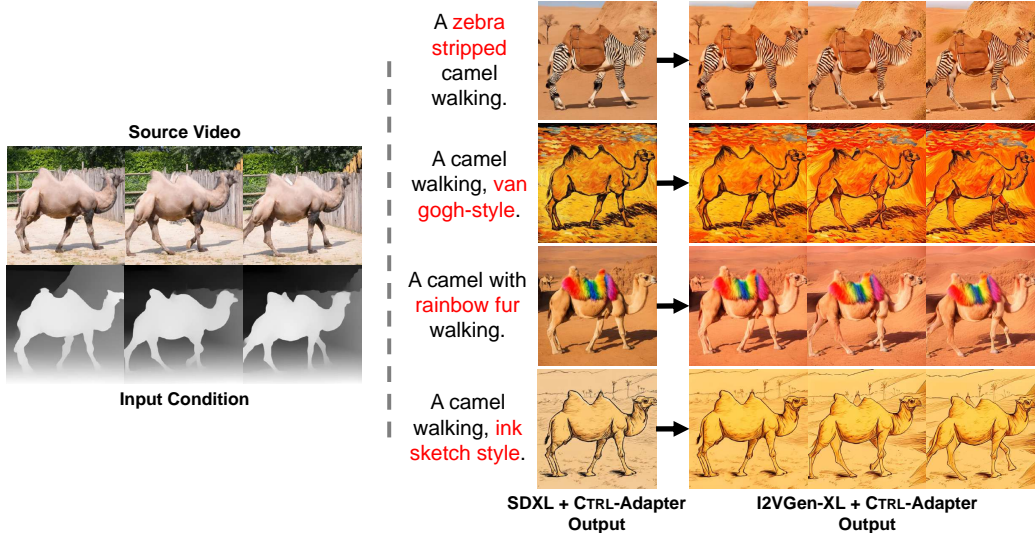


Figure 14: Video editing by combining SDXL and I2VGen-XL, where both models are equipped with spatial control via CTRL-Adapter. First, we extract conditions (e.g., depth map) from the original video. Next, we create the initial frame with SDXL + CTRL-Adapter. Lastly, we provide the newly generated initial frame and frame-wise conditions to I2VGen-XL + CTRL-Adapter to obtain the final edited video.

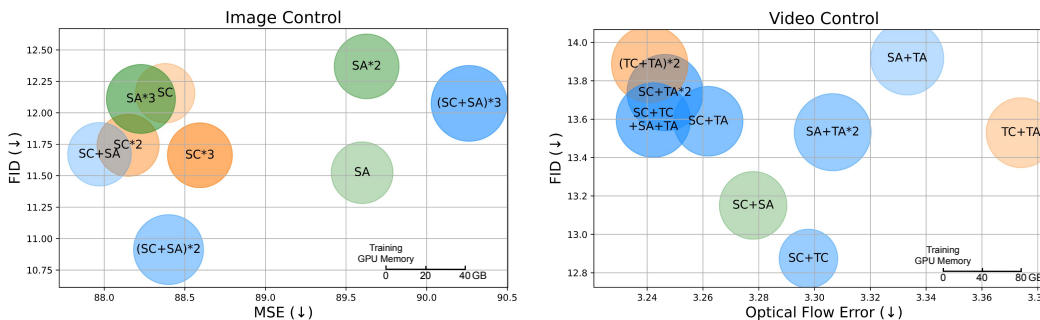


Figure 15: Comparison of different architecture of CTRL-Adapter for image and video control, measured with visual quality (FID) and spatial control (MSE/optical flow error) metrics. The metrics are calculated from 1000 randomly selected COCO val2017 images and 150 videos from DAVIS 2017 dataset respectively. **Left:** image control on SDXL backbone. **Right:** video control on I2VGen-XL backbone. For both plots, data points in the **bottom-left** are ideal. SC, TC, SA, and TA: Spatial Convolution, Temporal Convolution, Spatial Attention, and Temporal Attention. * N represents the number of blocks in each CTRL-Adapter. The diameters of bubbles represent peak training GPU memory.

improves temporal ability via a combination of temporal convolution and temporal attention. For **image control** (Fig. 15 left), we find that the combining of SC+SA is more effective than stacking SC or SA layers only. Stacking SC+SA twice further improves the visual quality (FID) slightly but hurts the spatial control (MSE) as a tradeoff. Stacking SC+SA three times hurts the performance due to insufficient training. We use the single SC+SA layer for image CTRL-Adapter by default. For **video control** (Fig. 15 right), we find that SC+TC+SA+TA shows the best balance of visual quality (FID) and spatial control (optical flow error). Notably, we find that the combinations with both temporal layers, SC+TC+SA+TA and (TC+TA)*2, achieve the lowest optical flow error. We use SC+TC+SA+TA for video CTRL-Adapter by default.

Table 5: Skipping latent from ControlNet inputs helps CTRL-Adapter for (1) adaptation to backbone models with different noise scales and (2) video control with sparse frame conditions.

Method	Latent z is given to ControlNet	Depth	
		FID (\downarrow)	Optical Flow Error (\downarrow)
Adaptation to different noise scales			
SVD [3] + CTRL-Adapter	✓	4.33	4.07
SVD [3] + CTRL-Adapter	✗	4.05	3.68
Sparse frame conditions			
I2VGen-XL [75] + CTRL-Adapter	✓	7.20	5.13
I2VGen-XL [75] + CTRL-Adapter	✗	5.98	4.88

6.2 Skipping Latent from ControlNet Inputs

As described in Sec. 3.2, we find skipping the latent z from ControlNet inputs can help CTRL-Adapter to more robustly handle (1) adaption to the backbone with noise scales different from SDv1.5, such as SVD and (2) video control with sparse frame conditions. Table 5 shows that skipping the latent z from ControlNet improves the visual quality (FID) and spatial control (optical flow error) metrics in both scenarios.

7 Conclusion

We propose CTRL-Adapter, an efficient and versatile framework that adds diverse controls to any image/video diffusion model, by adapting and temporally aligning pretrained ControlNets, while the parameters of the ControlNet and the backbone diffusion model are kept frozen. Training a CTRL-Adapter is significantly more efficient than training a ControlNet for a new backbone model. CTRL-Adapter also provides many useful capabilities including image control, video control, video control with sparse inputs, and multi-source controls. We empirically demonstrate the usefulness of CTRL-Adapter with comprehensive analysis. With diverse image and video diffusion backbones, training CTRL-Adapter can match or outperform training new ControlNets, while taking much lower computational cost. CTRL-Adapter perform zero-shot adaption to unseen conditions and help generate videos with sparse frame conditions or multiple conditions (*e.g.*, depth map, canny edge, human pose, and surface normal). We also provide comprehensive ablations for CTRL-Adapter design choices and qualitative examples. We hope our work can foster future works in efficient controlled generation of videos and images.

Acknowledgments

This work was supported by DARPA ECOLE Program No. HR00112390060, NSF-AI Engage Institute DRL-2112635, DARPA Machine Commonsense (MCS) Grant N66001-19-2-4031, ARO Award W911NF2110220, ONR Grant N00014-23-1-2356, and a Bloomberg Data Science Ph.D. Fellowship. The views contained in this article are those of the authors and not of the funding agency.

References

- [1] J. Ansel, E. Yang, H. He, N. Gimelshein, A. Jain, M. Voznesensky, B. Bao, P. Bell, D. Berard, E. Burovski, G. Chauhan, A. Chourdia, W. Constable, A. Desmaison, Z. DeVito, E. Ellison, W. Feng, J. Gong, M. Gschwind, B. Hirsh, S. Huang, K. Kalambarkar, L. Kirsch, M. Lazos, M. Lezcano, Y. Liang, J. Liang, Y. Lu, C. Luk, B. Maher, Y. Pan, C. Puhersch, M. Reso, M. Saroufim, M. Y. Siraichi, H. Suk, M. Suo, P. Tillet, E. Wang, X. Wang, W. Wen, S. Zhang, X. Zhao, K. Zhou, R. Zou, A. Mathews, G. Chanan, P. Wu, and S. Chintala. PyTorch 2: Faster Machine Learning Through Dynamic Python Bytecode Transformation and Graph Compilation. In *29th ACM International Conference on Architectural Support for Programming Languages and Operating Systems, Volume 2 (ASPLOS '24)*. ACM, Apr. 2024. 6, 22
- [2] O. Avrahami, T. Hayes, O. Gafni, S. Gupta, Y. Taigman, D. Parikh, D. Lischinski, O. Fried, and X. Yin. SpaText: Spatio-Textual Representation for Controllable Image Generation. In *CVPR*, nov 2023. 2, 3
- [3] A. Blattmann, T. Dockhorn, S. Kulal, D. Mendeleevitch, M. Kilian, D. Lorenz, Y. Levi, Z. English, V. Voleti, A. Letts, et al. Stable video diffusion: Scaling latent video diffusion models to large datasets. *arXiv preprint arXiv:2311.15127*, 2023. 2, 3, 6, 7, 9, 17, 22

- [4] G. Bradski. The OpenCV Library. *Dr. Dobb's Journal of Software Tools*, 2000. 7
- [5] Z. Cao, T. Simon, S.-E. Wei, and Y. Sheikh. Realtime multi-person 2d pose estimation using part affinity fields. In *Proceedings of the IEEE conference on computer vision and pattern recognition*, pages 7291–7299, 2017. 7
- [6] H. Chen, Y. Zhang, X. Cun, M. Xia, X. Wang, C. Weng, and Y. Shan. Videocrafter2: Overcoming data limitations for high-quality video diffusion models, 2024. 2
- [7] T.-S. Chen, A. Siarohin, W. Menapace, E. Deyneka, H.-w. Chao, B. E. Jeon, Y. Fang, H.-Y. Lee, J. Ren, M.-H. Yang, and S. Tulyakov. Panda-70m: Captioning 70m videos with multiple cross-modality teachers. In *CVPR 2024*, 2024. 7
- [8] W. Chen, J. Wu, P. Xie, H. Wu, J. Li, X. Xia, X. Xiao, and L. Lin. Control-a-video: Controllable text-to-video generation with diffusion models. *arXiv preprint arXiv:2305.13840*, 2023. 8, 9
- [9] X. Dai, J. Hou, C.-Y. Ma, S. Tsai, J. Wang, R. Wang, P. Zhang, S. Vandenhende, X. Wang, A. Dubey, et al. Emu: Enhancing image generation models using photogenic needles in a haystack. *arXiv preprint arXiv:2309.15807*, 2023. 7
- [10] P. Esser, S. Kulal, A. Blattmann, R. Entezari, J. Müller, H. Saini, Y. Levi, D. Lorenz, A. Sauer, F. Boesel, D. Podell, T. Dockhorn, Z. English, K. Lacey, A. Goodwin, Y. Marek, and R. Rombach. Scaling rectified flow transformers for high-resolution image synthesis, 2024. 6
- [11] G. Farneböck. Two-frame motion estimation based on polynomial expansion. In *Image Analysis: 13th Scandinavian Conference, SCIA 2003 Halmstad, Sweden, June 29–July 2, 2003 Proceedings 13*, pages 363–370. Springer, 2003. 7
- [12] G. Farneböck. Two-frame motion estimation based on polynomial expansion. In *Scandinavian Conference on Image Analysis*, 2003. 7
- [13] O. Gafni, A. Polyak, O. Ashual, S. Sheynin, D. Parikh, and Y. Taigman. Make-A-Scene: Scene-Based Text-to-Image Generation with Human Priors. In *ECCV*, 2022. 2, 3
- [14] R. Gal, Y. Alaluf, Y. Atzmon, O. Patashnik, A. H. Bermano, G. Chechik, and D. Cohen-Or. An Image is Worth One Word: Personalizing Text-to-Image Generation using Textual Inversion. In *ICLR*, 2023. 2, 3
- [15] R. Girdhar, M. Singh, A. Brown, Q. Duval, S. Azadi, S. S. Rambhatla, A. Shah, X. Yin, D. Parikh, and I. Misra. Emu video: Factorizing text-to-video generation by explicit image conditioning. *arXiv preprint arXiv:2311.10709*, 2023. 2
- [16] I. Goodfellow, J. Pouget-Abadie, M. Mirza, B. Xu, D. Warde-Farley, S. Ozair, A. Courville, and Y. Bengio. Generative adversarial networks. *Communications of the ACM*, 63(11):139–144, 2020. 3
- [17] Y. Guo, C. Yang, A. Rao, M. Agrawala, D. Lin, and B. Dai. Sparsectrl: Adding sparse controls to text-to-video diffusion models. *arXiv preprint arXiv:2311.16933*, 2023. 3, 4, 23
- [18] Y. Guo, C. Yang, A. Rao, Y. Wang, Y. Qiao, D. Lin, and B. Dai. Animatediff: Animate your personalized text-to-image diffusion models without specific tuning. In *International Conference on Learning Representations*, 2024. 3
- [19] A. Gupta, L. Yu, K. Sohn, X. Gu, M. Hahn, L. Fei-Fei, I. Essa, L. Jiang, and J. Lezama. Photorealistic video generation with diffusion models, 2023. 3
- [20] K. He, X. Zhang, S. Ren, and J. Sun. Deep residual learning for image recognition. In *2016 IEEE Conference on Computer Vision and Pattern Recognition (CVPR)*, pages 770–778, 2016. 15
- [21] Y. He, T. Yang, Y. Zhang, Y. Shan, and Q. Chen. Latent video diffusion models for high-fidelity long video generation, 2022. 3
- [22] M. Heusel, H. Ramsauer, T. Unterthiner, B. Nessler, and S. Hochreiter. Gans trained by a two time-scale update rule converge to a local nash equilibrium. *Advances in neural information processing systems*, 30, 2017. 8
- [23] J. Ho, W. Chan, C. Saharia, J. Whang, R. Gao, A. Gritsenko, D. P. Kingma, B. Poole, M. Norouzi, D. J. Fleet, et al. Imagen video: High definition video generation with diffusion models. *arXiv preprint arXiv:2210.02303*, 2022. 3
- [24] J. Ho, A. Jain, and P. Abbeel. Denoising diffusion probabilistic models. *Advances in neural information processing systems*, 33:6840–6851, 2020. 3, 5

- [25] E. Hoogeboom, J. Heek, and T. Salimans. simple diffusion: End-to-end diffusion for high resolution images. In *International Conference on Machine Learning*, pages 13213–13232. PMLR, 2023. 6
- [26] N. Houlsby, A. Giurgiu, S. Jastrzebski, B. Morrone, Q. de Laroussilhe, A. Gesmundo, M. Attariyan, and S. Gelly. Parameter-efficient transfer learning for nlp. In *ICML*, volume abs/1902.00751, 2019. 2
- [27] Z. Hu and D. Xu. Videocontrolnet: A motion-guided video-to-video translation framework by using diffusion model with controlnet. *arXiv preprint arXiv:2307.14073*, 2023. 4, 8, 9
- [28] L. Khachatryan, A. Movsisyan, V. Tadevosyan, R. Henschel, Z. Wang, S. Navasardyan, and H. Shi. Text2video-zero: Text-to-image diffusion models are zero-shot video generators. In *ICCV 2023*, 2023. 3, 8, 9
- [29] S. Kim, J. Lee, K. Hong, D. Kim, and N. Ahn. Diffblender: Scalable and composable multimodal text-to-image diffusion models. *arXiv preprint arXiv:2305.15194*, 2023. 3
- [30] D. P. Kingma and M. Welling. Auto-encoding variational bayes. In *ICLR*, 2014. 3
- [31] D. Li, J. Li, and S. C. H. Hoi. BLIP-Diffusion: Pre-trained Subject Representation for Controllable Text-to-Image Generation and Editing. In *NeurIPS*, 2023. 2, 3
- [32] Y. Li, Z. Gan, Y. Shen, J. Liu, Y. Cheng, Y. Wu, L. Carin, D. Carlson, and J. Gao. Storygan: A sequential conditional gan for story visualization. In *CVPR*, 2019. 3
- [33] Y. Li, H. Liu, Q. Wu, F. Mu, J. Yang, J. Gao, C. Li, and Y. J. Lee. Gligen: Open-set grounded text-to-image generation. In *Proceedings of the IEEE/CVF Conference on Computer Vision and Pattern Recognition*, pages 22511–22521, 2023. 2, 3, 10
- [34] Y. Li, M. R. Min, D. Shen, D. Carlson, and L. Carin. Video generation from text. In *AAAI*, 2017. 3
- [35] H. Lin, A. Zala, J. Cho, and M. Bansal. Videodirectorgpt: Consistent multi-scene video generation via llm-guided planning. *arXiv preprint arXiv:2309.15091*, 2023. 2
- [36] T.-Y. Lin, M. Maire, S. Belongie, J. Hays, P. Perona, D. Ramanan, P. Dollár, and C. L. Zitnick. Microsoft coco: Common objects in context. In *Computer Vision—ECCV 2014: 13th European Conference, Zurich, Switzerland, September 6–12, 2014, Proceedings, Part V 13*, pages 740–755. Springer, 2014. 3, 8
- [37] F. Long, Z. Qiu, T. Yao, and T. Mei. Videodrafter: Content-consistent multi-scene video generation with llm. *arXiv preprint arXiv:2401.01256*, 2024. 2
- [38] N. Ma, M. Goldstein, M. S. Albergo, N. M. Boffi, E. Vanden-Eijnden, and S. Xie. Sit: Exploring flow and diffusion-based generative models with scalable interpolant transformers. *arXiv preprint arXiv:2401.08740*, 2024. 6
- [39] W. Menapace, A. Siarohin, I. Skorokhodov, E. Deyneka, T.-S. Chen, A. Kag, Y. Fang, A. Stoliar, E. Ricci, J. Ren, and S. Tulyakov. Snap video: Scaled spatiotemporal transformers for text-to-video synthesis, 2024. 3
- [40] C. Mou, X. Wang, L. Xie, Y. Wu, J. Zhang, Z. Qi, Y. Shan, and X. Qie. T2i-adapter: Learning adapters to dig out more controllable ability for text-to-image diffusion models. In *AAAI 2024*, 2023. 3, 10
- [41] J. Mullan, D. Crawbuck, and A. Sastry. Hotshot-XL, Oct. 2023. 3, 7, 9
- [42] OpenAI. Video generation models as world simulators, 2024. 3
- [43] G. Parmar, R. Zhang, and J.-Y. Zhu. On aliased resizing and surprising subtleties in gan evaluation. In *CVPR*, 2022. 9
- [44] D. Podell, Z. English, K. Lacey, A. Blattmann, T. Dockhorn, J. Müller, J. Penna, and R. Rombach. Sdxl: Improving latent diffusion models for high-resolution image synthesis. In *International Conference on Learning Representations*, 2024. 2, 3, 5, 7
- [45] J. Pont-Tuset, F. Perazzi, S. Caelles, P. Arbeláez, A. Sorkine-Hornung, and L. Van Gool. The 2017 davis challenge on video object segmentation. *arXiv preprint arXiv:1704.00675*, 2017. 3, 8
- [46] C. Qin, S. Zhang, N. Yu, Y. Feng, X. Yang, Y. Zhou, H. Wang, J. C. Niebles, C. Xiong, S. Savarese, et al. Unicontrol: A unified diffusion model for controllable visual generation in the wild. In *NeurIPS 2023*, 2023. 3, 4, 8

- [47] A. Ramesh, P. Dhariwal, A. Nichol, C. Chu, and M. Chen. Hierarchical Text-Conditional Image Generation with CLIP Latents, 2022. 2
- [48] L. Ran, X. Cun, J.-W. Liu, R. Zhao, S. Zijie, X. Wang, J. Keppo, and M. Z. Shou. X-adapter: Adding universal compatibility of plugins for upgraded diffusion model. In *CVPR*, 2024. 3, 7, 10, 11, 15, 23
- [49] R. Ranftl, K. Lasinger, D. Hafner, K. Schindler, and V. Koltun. Towards robust monocular depth estimation: Mixing datasets for zero-shot cross-dataset transfer. *IEEE transactions on pattern analysis and machine intelligence*, 44(3):1623–1637, 2020. 7
- [50] A. Ranjan and M. J. Black. Optical flow estimation using a spatial pyramid network. In *Proceedings of the IEEE conference on computer vision and pattern recognition*, pages 4161–4170, 2017. 8
- [51] R. Rombach, A. Blattmann, D. Lorenz, P. Esser, and B. Ommer. High-resolution image synthesis with latent diffusion models. *2022 IEEE/CVF Conference on Computer Vision and Pattern Recognition (CVPR)*, pages 10674–10685, 2021. 6
- [52] R. Rombach, A. Blattmann, D. Lorenz, P. Esser, and B. Ommer. High-resolution image synthesis with latent diffusion models. In *Proceedings of the IEEE/CVF conference on computer vision and pattern recognition*, pages 10684–10695, 2022. 2, 5
- [53] C. Rowles. Stable Video Diffusion Temporal Controlnet. <https://github.com/CiaraStrawberry/svd-temporal-controlnet>, 2023. 8, 9
- [54] N. Ruiz, Y. Li, V. Jampani, Y. Pritch, M. Rubinstein, and K. Aberman. DreamBooth: Fine Tuning Text-to-Image Diffusion Models for Subject-Driven Generation. In *CVPR*, 2023. 2, 3
- [55] S. Ryu. Low-rank adaptation for fast text-to-image diffusion fine-tuning, 2022. 3
- [56] C. Saharia, W. Chan, S. Saxena, L. Li, J. Whang, E. Denton, S. K. S. Ghasemipour, B. K. Ayan, S. S. Mahdavi, R. G. Lopes, T. Salimans, J. Ho, D. J. Fleet, and M. Norouzi. Photorealistic Text-to-Image Diffusion Models with Deep Language Understanding. In *NeurIPS*, 2022. 2
- [57] C. Schuhmann, R. Beaumont, R. Vencu, C. Gordon, R. Wightman, M. Cherti, T. Coombes, A. Katta, C. Mullis, M. Wortsman, et al. Laion-5b: An open large-scale dataset for training next generation image-text models. *Advances in Neural Information Processing Systems*, 35:25278–25294, 2022. 7
- [58] N. Shazeer, A. Mirhoseini, K. Maziarz, A. Davis, Q. Le, G. Hinton, and J. Dean. Outrageously Large Neural Networks: the Sparsely-Gated Mixture-of-Experts Layer. In *ICLR*, 2017. 6
- [59] U. Singer, A. Polyak, T. Hayes, X. Yin, J. An, S. Zhang, Q. Hu, H. Yang, O. Ashual, O. Gafni, et al. Make-a-video: Text-to-video generation without text-video data. In *ICLR*, 2023. 3
- [60] I. Skorokhodov, S. Tulyakov, and M. Elhoseiny. Stylegan-v: A continuous video generator with the price, image quality and perks of stylegan2. In *CVPR*, 2022. 3
- [61] J. Sohl-Dickstein, E. A. Weiss, N. Maheswaranathan, and S. Ganguli. Deep unsupervised learning using nonequilibrium thermodynamics. In *ICML*, 2015. 3
- [62] P. von Platen, S. Patil, A. Lozhkov, P. Cuenca, N. Lambert, K. Rasul, M. Davaadorj, and T. Wolf. Diffusers: State-of-the-art diffusion models. <https://github.com/huggingface/diffusers>, 2022. 8, 10, 11
- [63] F.-Y. Wang, W. Chen, G. Song, H.-J. Ye, Y. Liu, and H. Li. Gen-l-video: Multi-text to long video generation via temporal co-denoising. *arXiv preprint arXiv:2305.18264*, 2023. 3
- [64] J. Wang, H. Yuan, D. Chen, Y. Zhang, X. Wang, and S. Zhang. Modelscope text-to-video technical report, 2023. 3
- [65] W. Wang, Q. Lv, W. Yu, W. Hong, J. Qi, Y. Wang, J. Ji, Z. Yang, L. Zhao, X. Song, et al. Cogvlm: Visual expert for pretrained language models. *arXiv preprint arXiv:2311.03079*, 2023. 7
- [66] X. Wang, H. Yuan, S. Zhang, D. Chen, J. Wang, Y. Zhang, Y. Shen, D. Zhao, and J. Zhou. Videocomposer: Compositional video synthesis with motion controllability. *Advances in Neural Information Processing Systems*, 36, 2024. 3, 8, 9, 15
- [67] Z. Wang, A. C. Bovik, H. R. Sheikh, and E. P. Simoncelli. Image quality assessment: from error visibility to structural similarity. *IEEE transactions on image processing*, 13(4):600–612, 2004. 8
- [68] T. Xiao, Y. Liu, B. Zhou, Y. Jiang, and J. Sun. Unified perceptual parsing for scene understanding. In *Proceedings of the European conference on computer vision (ECCV)*, pages 418–434, 2018. 7

- [69] E. Xie, W. Wang, Z. Yu, A. Anandkumar, J. M. Alvarez, and P. Luo. Segformer: Simple and efficient design for semantic segmentation with transformers. *Advances in Neural Information Processing Systems*, 34:12077–12090, 2021. [7](#)
- [70] J. Xing, M. Xia, Y. Zhang, H. Chen, W. Yu, H. Liu, X. Wang, T.-T. Wong, and Y. Shan. Dynamicrafter: Animating open-domain images with video diffusion priors. *arXiv preprint arXiv:2310.12190*, 2023. [3](#)
- [71] Z. Yang, J. Wang, Z. Gan, L. Li, K. Lin, C. Wu, N. Duan, Z. Liu, C. Liu, M. Zeng, and L. Wang. Reco: Region-controlled text-to-image generation. In *Proceedings of the IEEE/CVF Conference on Computer Vision and Pattern Recognition*, 2023. [2](#), [3](#)
- [72] M. B. Yi-Lin Sung, Jaemin Cho. Vi-adapter: Parameter-efficient transfer learning for vision-and-language tasks. In *CVPR*, 2022. [2](#)
- [73] S. Yin, C. Wu, H. Yang, J. Wang, X. Wang, M. Ni, Z. Yang, L. Li, S. Liu, F. Yang, J. Fu, M. Gong, L. Wang, Z. Liu, H. Li, and N. Duan. NUWA-XL: Diffusion over diffusion for eXtremely long video generation. In *Proceedings of the 61st Annual Meeting of the Association for Computational Linguistics (Volume 1: Long Papers)*, pages 1309–1320, Toronto, Canada, July 2023. Association for Computational Linguistics. [3](#)
- [74] L. Zhang, A. Rao, and M. Agrawala. Adding conditional control to text-to-image diffusion models. In *Proceedings of the IEEE/CVF International Conference on Computer Vision*, pages 3836–3847, 2023. [2](#), [3](#), [4](#), [5](#), [7](#), [10](#)
- [75] S. Zhang, J. Wang, Y. Zhang, K. Zhao, H. Yuan, Z. Qin, X. Wang, D. Zhao, and J. Zhou. I2vgen-xl: High-quality image-to-video synthesis via cascaded diffusion models. *arXiv preprint arXiv:2311.04145*, 2023. [3](#), [5](#), [7](#), [9](#), [17](#)
- [76] Y. Zhang, Y. Wei, D. Jiang, X. Zhang, W. Zuo, and Q. Tian. Controlvideo: Training-free controllable text-to-video generation. In *ICLR*, 2024. [4](#), [8](#), [9](#)
- [77] L. Zhao, X. Peng, Y. Tian, M. Kapadia, and D. Metaxas. Learning to forecast and refine residual motion for image-to-video generation. In *Proceedings of the European Conference on Computer Vision (ECCV)*, September 2018. [3](#)
- [78] S. Zhao, D. Chen, Y.-C. Chen, J. Bao, S. Hao, L. Yuan, and K.-Y. K. Wong. Uni-controlnet: All-in-one control to text-to-image diffusion models. *Advances in Neural Information Processing Systems*, 36, 2024. [3](#), [8](#), [9](#), [10](#), [11](#)
- [79] D. Zhou, W. Wang, H. Yan, W. Lv, Y. Zhu, and J. Feng. Magicvideo: Efficient video generation with latent diffusion models. *arXiv preprint arXiv:2211.11018*, 2022. [3](#)

Appendix

In this appendix, we include PyTorch implementation for inverse timestep sampling (Appendix A), CTRL-Adapter architecture details (Appendix B), comparison of CTRL-Adapter variants and related methods (Appendix C), additional quantitative analysis (Appendix D), and additional qualitative examples (Appendix E).

A PyTorch Implementation for Inverse Timestep Sampling

In Algorithm 1, we provide the PyTorch [1] implementation of inverse timestep sampling, described in Sec. 3.2. In the example, inverse time stamping is used to adapt to the SVD [3] backbone.

Algorithm 1 PyTorch Implementation for Inverse Timestep Sampling

```
import torch

def sample_sigma(u, loc=0., scale=1.):
    """Draw a noise scale (sigma) from a pre-defined distribution.
    Here, we use lognormal distribution used in SVD."""
    return torch.distributions.Normal(loc, scale).icdf(u).exp()

def sigma_to_timestep(sigma):
    """Map noise scale to timestep.
    Here, we use the function used in SVD."""
    timestep = 0.25 * sigma.log()
    return timestep

def inverse_timestep_sample():
    """Sample noise scales and timesteps for ControlNet and diffusion models
    trained with continuous noise sampler. Here, we use the setting used for SVD.
    """
    # 1) sample u from Uniform[0,1]
    u = torch.rand(1)
    # 2) calculate sigma_svd from pre-defined log-normal distribution
    sigma_svd = sample_sigma(u, loc=0.7, scale=1.6)
    # 3) calculate timestep_svd from sigma_svd via pre-defined mapping function
    timestep_svd = sigma_to_timestep(sigma_svd)
    # 4) calculate timestep and sigma for controlnet
    sigma_cnet, timestep_cnet = u, int(1000 * u)
    return sigma_svd, timestep_svd, sigma_cnet, timestep_cnet
```

B CTRL-Adapter Architecture Details

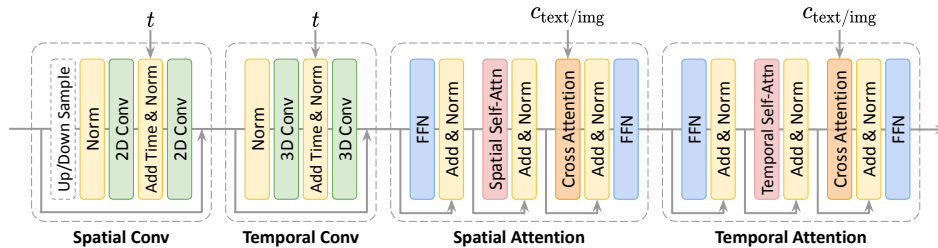


Figure 16: Detailed architecture of CTRL-Adapter blocks.

In Fig. 16, we illustrate the detailed architecture of CTRL-Adapter blocks. See Fig. 2 for how the CTRL-Adapter blocks are used to adapt ControlNets to image/video diffusion models. We extend the Fig. 2 with adding more detailed visualizations, including skip connections, normalization layers in each module, and the linear projection layers (*i.e.*, FFN) in each spatial/temporal attention modules.

C Comparison of CTRL-Adapter Variants and Related Methods

In Fig. 17, we compare the variants of CTRL-Adapter designs (with latent is given / not given to ControlNet; see Sec. 3.2 for details) and two related methods: SparseCtrl [17] and X-Adapter [48]. Unlike CTRL-Adapter that leverages the pretrained image ControlNets, SparseCtrl (Fig. 17 c) trains a video ControlNet with control conditions c_f and frame masks m as inputs. While X-Adapter (Fig. 17 d) needs SDv1.5 UNet as well as SDv1.5 ControlNet during training and inference, CTRL-Adapter doesn't need to SDv1.5 UNet at all.

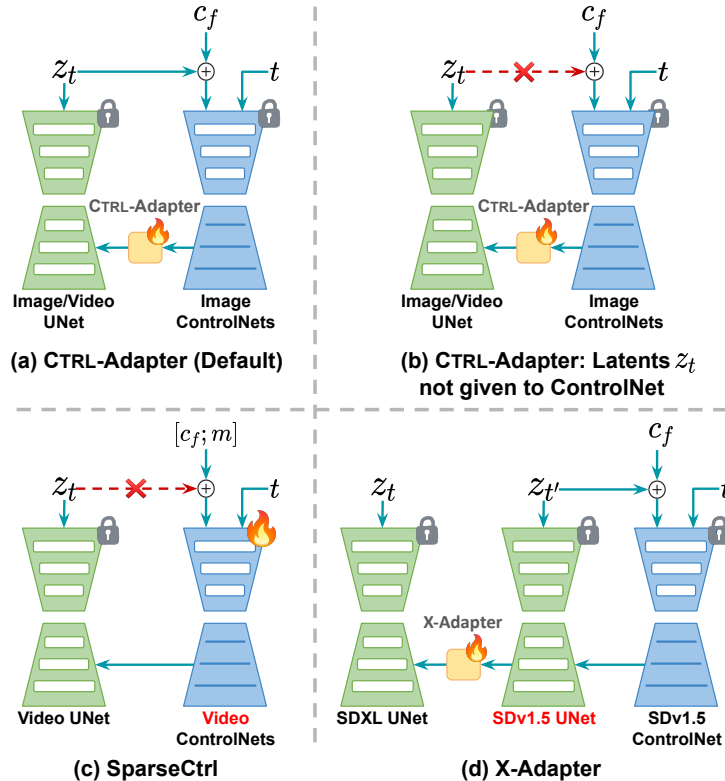


Figure 17: Comparison of giving different inputs to ControlNet, where z_t , c_f , and t represent latents, input control features, and timesteps respectively. **(a):** Default CTRL-Adapter design. **(b):** Variant of CTRL-Adapter where latents z_t are not given to ControlNet (see Sec. 3.2 for details). **(c):** SparseCtrl [17] trains a video ControlNet with control conditions c_f and frame masks m as inputs. **(d):** X-Adapter [48] needs SDv1.5 UNet as well as SDv1.5 ControlNet during training and inference, whereas CTRL-Adapter doesn't need to SDv1.5 UNet at all.

D Additional Quantitative Analysis

D.1 CTRL-Adapter Design Ablations

Where to fuse CTRL-Adapter outputs in backbone diffusion. We compare the integration of CTRL-Adapter outputs at different positions of video diffusion backbone model. As illustrated in Fig. 2, we experiment with integrating CTRL-Adapter outputs to different positions of I2VGen-XL's UNet: middle block, output block A, output block B, output block C, and output block D. Specifically, we compared our default design (Mid + Out ABCD) with four other variants (Out ABCD, Out ABC, Out AB, and Out A) that gradually remove CTRL-Adapters from the middle block and output blocks at positions from B to D. As shown in Fig. 18, removing the CTRL-Adapters from the middle block and the output block D does not lead to a noticeable increase in FID or optical flow error (*i.e.*, the performances of 'Mid+Out ABCD', 'Out ABCD', and 'Out ABC' are similar in both left and right plots). However, Fig. 18 (right) shows that continuing to remove CTRL-Adapters from block C causes

a significant increase in optical flow error. Therefore, we recommend users retain our CTRL-Adapters in the mid block and output blocks A, B, and C to maintain optimal performance.

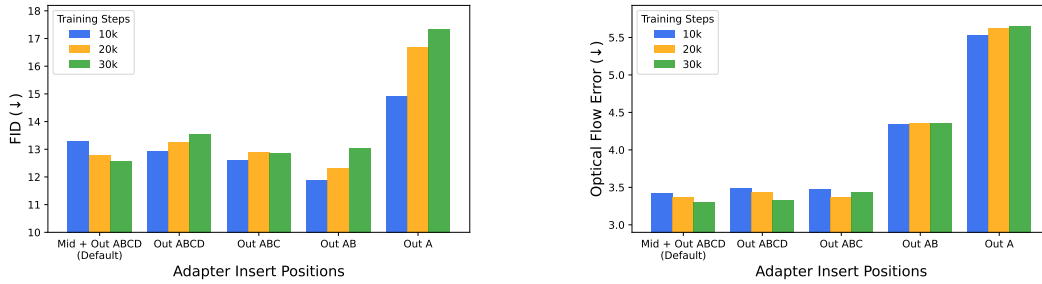


Figure 18: Comparison of inserting CTRL-Adapter to different UNet blocks. ‘Mid’ represents the middle block, whereas ‘Out ABCD’ represents output blocks A, B, C, and D. The metrics are calculated from 150 videos from DAVIS 2017 dataset.

Number of CTRL-Adapters in each output block position. As illustrated in Fig. 2, there are three output blocks for each feature map dimension in the video diffusion model (represented by $\times 3$ in each output block). Here, we conduct an ablation study by adding CTRL-Adapters to only one or two of the three output blocks of the same feature size. The motivation is that using fewer CTRL-Adapters can almost linearly decrease the number of trainable parameters, thereby reducing GPU memory usage during training. We visualize the architectural changes with output block D as an example in Fig. 19. We insert CTRL-Adapters for three blocks as our default setting. As observed in Fig. 20, reducing the number of CTRL-Adapters increases the optical flow error. Therefore, we recommend adding CTRL-Adapters to each output block to maintain optimal performance.

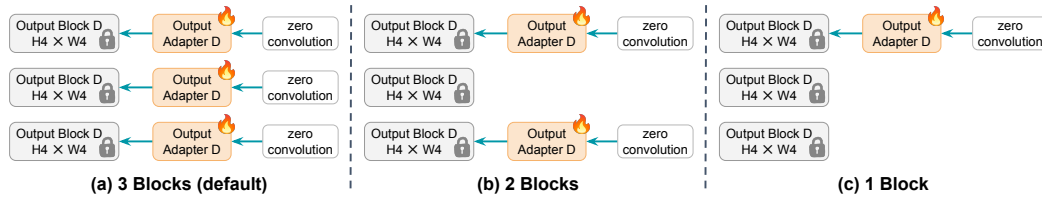


Figure 19: Comparison of inserting different numbers of CTRL-Adapters from the ControlNet’s zero-convolution layers to the backbone diffusion UNet’s output blocks. We use output block D here as an example. We insert three CTRL-Adapters to three output blocks of the same feature map size by default.

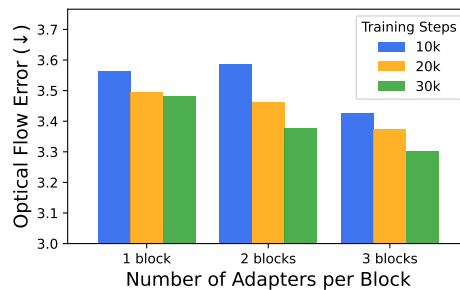


Figure 20: Comparison of inserting different numbers of CTRL-Adapters to each UNet output block. The metrics are calculated from 150 videos from DAVIS 2017 dataset. We insert 3 CTRL-Adapters to each output block by default.

D.2 Trade-off between Visual Quality and Spatial Control

In Fig. 21, Fig. 22, and Fig. 23, we show the visual quality (FID) and spatial control (SSIM/optical flow error) metrics with different numbers of denoising steps with spatial control (with the fusion of CTRL-Adapter outputs) on SDXL, SVD, and I2VGen-XL backbones respectively. Specifically, suppose we use N denoising steps during inference, a control guidance level of $x\%$ means that we fuse CTRL-Adapter features to the video diffusion UNet during the first $x\% \times N$ denoising steps, followed by $(100 - x)\% \times N$ regular denoising steps. In all experiments, we find that increasing the number of denoising steps with spatial control improves the spatial control accuracies (SSIM/optical flow error) but hurts visual quality (FID).

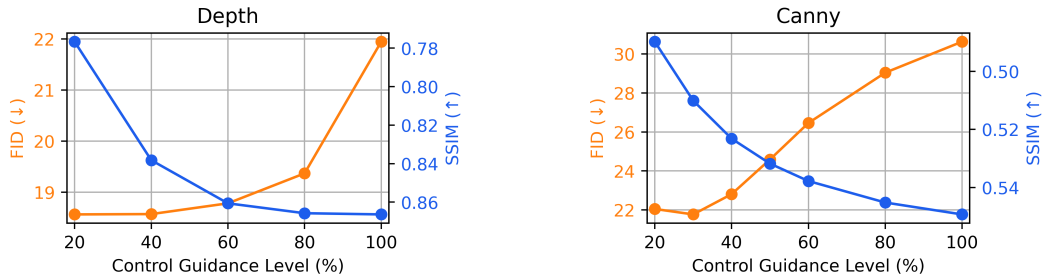


Figure 21: Trade-off between generated visual quality (FID) and spatial control accuracy (SSIM) on **SDXL**. Control guidance level of x represents that we apply CTRL-Adapter in the first $x\%$ of the denoising steps during inference. A control guidance level between 30% and 60% usually achieves the best balance between image quality and spatial control accuracy.

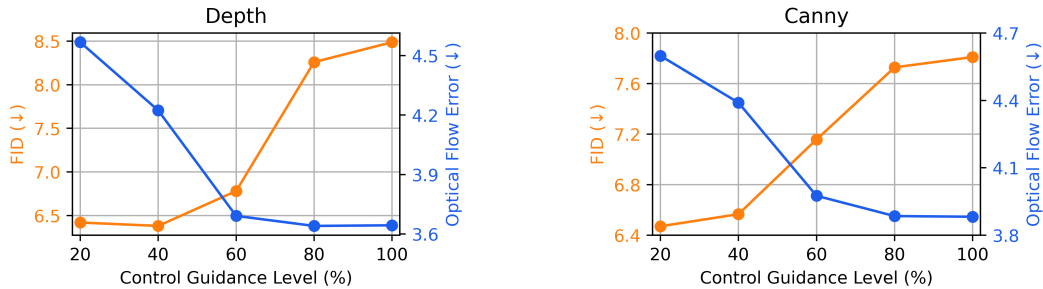


Figure 22: Trade-off between generated visual quality (FID) and spatial control accuracy (Optical Flow Error) on **SVD**. Control guidance level of x represents that we apply CTRL-Adapter in the first $x\%$ of the denoising steps during inference. A control guidance level between 40% and 60% usually achieves the best balance between image quality and spatial control accuracy

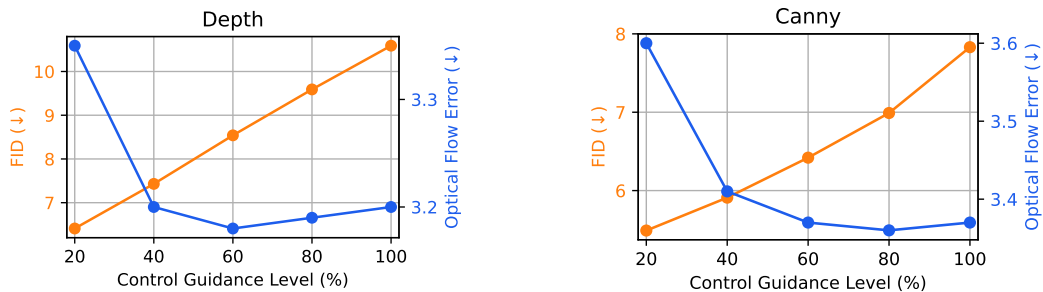


Figure 23: Trade-off between generated visual quality (FID) and spatial control accuracy (Optical Flow Error) on **I2VGen-XL**. Control guidance level of x represents that we apply CTRL-Adapter in the first $x\%$ of the denoising steps during inference. A control guidance level between 40% and 60% usually achieves the best balance between image quality and spatial control accuracy.

Table 6: Comparison of different weighting methods for multi-condition video generation (see Fig. 24 for visualization of the weighting methods). The control sources are abbreviated as D (depth map), C (canny edge), N (surface normal), S (softedge), Seg (semantic segmentation map), L (line art), and P (human pose).

Conditions	Equal Weights		Linear Weights (Default)		MLP Router					
	FID (\downarrow)	Flow Error (\downarrow)	FID (\downarrow)	Flow Error (\downarrow)	Timestep		Text/Image Emb		Timestep+Text/Image Emb	
					FID (\downarrow)	Flow Error (\downarrow)	FID (\downarrow)	Flow Error (\downarrow)	FID (\downarrow)	Flow Error (\downarrow)
D + C	8.50	2.84	9.14	2.89	9.41	3.51	8.73	3.16	8.64	3.31
D + P	11.32	3.48	10.98	3.32	11.13	3.35	11.35	3.37	10.69	3.43
D + C + N + S	8.75	2.40	8.39	2.23	9.51	2.78	7.91	2.76	8.09	2.69
D + C + N + S + Seg + L + P	9.48	2.93	8.18	2.48	8.17	2.45	8.83	2.48	8.51	2.43

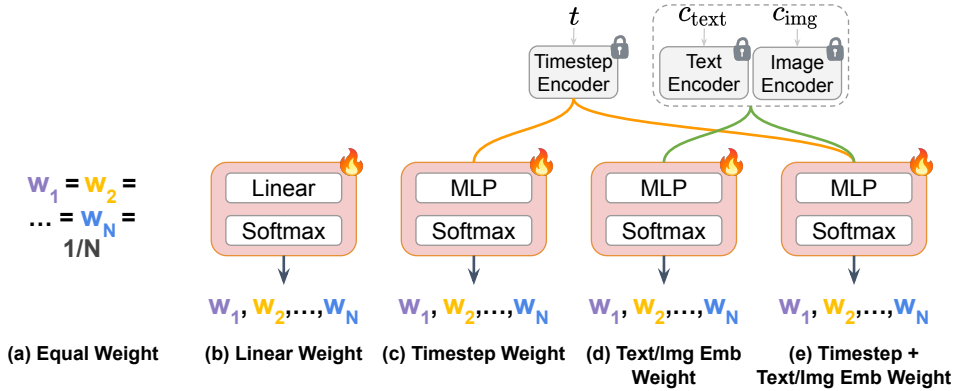


Figure 24: Visualization of different routing methods for combining multiple ControlNet outputs.

D.3 Different weighing modules for multi-condition generation

For multi-condition generation described in Sec. 3.3, in addition to simple linear weights, we also experimented with learning a router module that takes additional inputs such as diffusion time steps and image/text embeddings and outputs weights for different ControlNets. We compare (a) equal weights; (b) linear weights, learning a scalar weight to each ControlNet CTRL-Adapter; (c) MLP router - taking timestep as inputs; (d) MLP router - taking image/text embedding as inputs; and (e) MLP router - taking timestep and image/text embedding as inputs. The MoE router in (c), (d), (e) are constructed as a 3-layer MLP. We illustrate the five methods in Fig. 24.

All weighting schemes perform effectively. Table 6 show that all weighting schemes for fusing different ControlNet outputs perform effectively, and no specific method outperforms other methods with significant margins in all settings. Thus, we use a single linear weighting scheme as our default configuration for multi-condition generation.

Visualization of learned weight for different conditions. In Fig. 25, we illustrate the learned linear weights allocated to each control condition in each of the middle and output blocks of CTRL-Adapter on the I2VGen-XL backbone.

E Additional Qualitative Examples

We provide additional qualitative examples in the following.

In Fig. 26 and Fig. 27, we show image generation results on COCO val2017 split using depth map and canny edge conditions, respectively.

In Fig. 28 and Fig. 29, we show video generation results on depth map and canny edges extracted from videos from Sora¹¹ and videos from the internet, using depth map and canny edge conditions, respectively.

¹¹<https://openai.com/sora>

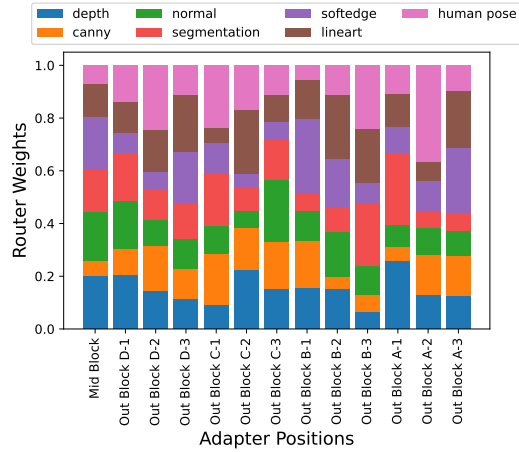


Figure 25: Linear weights allocated to each control condition in each of the middle and output blocks of CTRL-Adapter on the I2VGen-XL backbone.

In Fig. 30 and Fig. 31, we show image generation results on prompts from Lexica¹² using depth map and canny edge conditions, respectively.

¹²<https://lexica.art/>

Input Prompt	Input Depth Map	SDXL ControlNet	X-Adapter	CTRL-Adapter (Ours)
A police officer on a motorcycle drives through a parade.				
A middle aged black woman is standing behind a table full of bananas.				
A pair of children stand on a fence together				
A man sitting in a restaurant photographs a sandwich.				
A man in a reception hall holds a drink				
A woman is skiing down a snowy hill				
A vegetable vendor organizing his food for sale				

Figure 26: Image generation results on COCO val2017 split using **depth map** as control condition.



Figure 27: Image generation results on COCO val2017 split using **canny edge** as control condition.

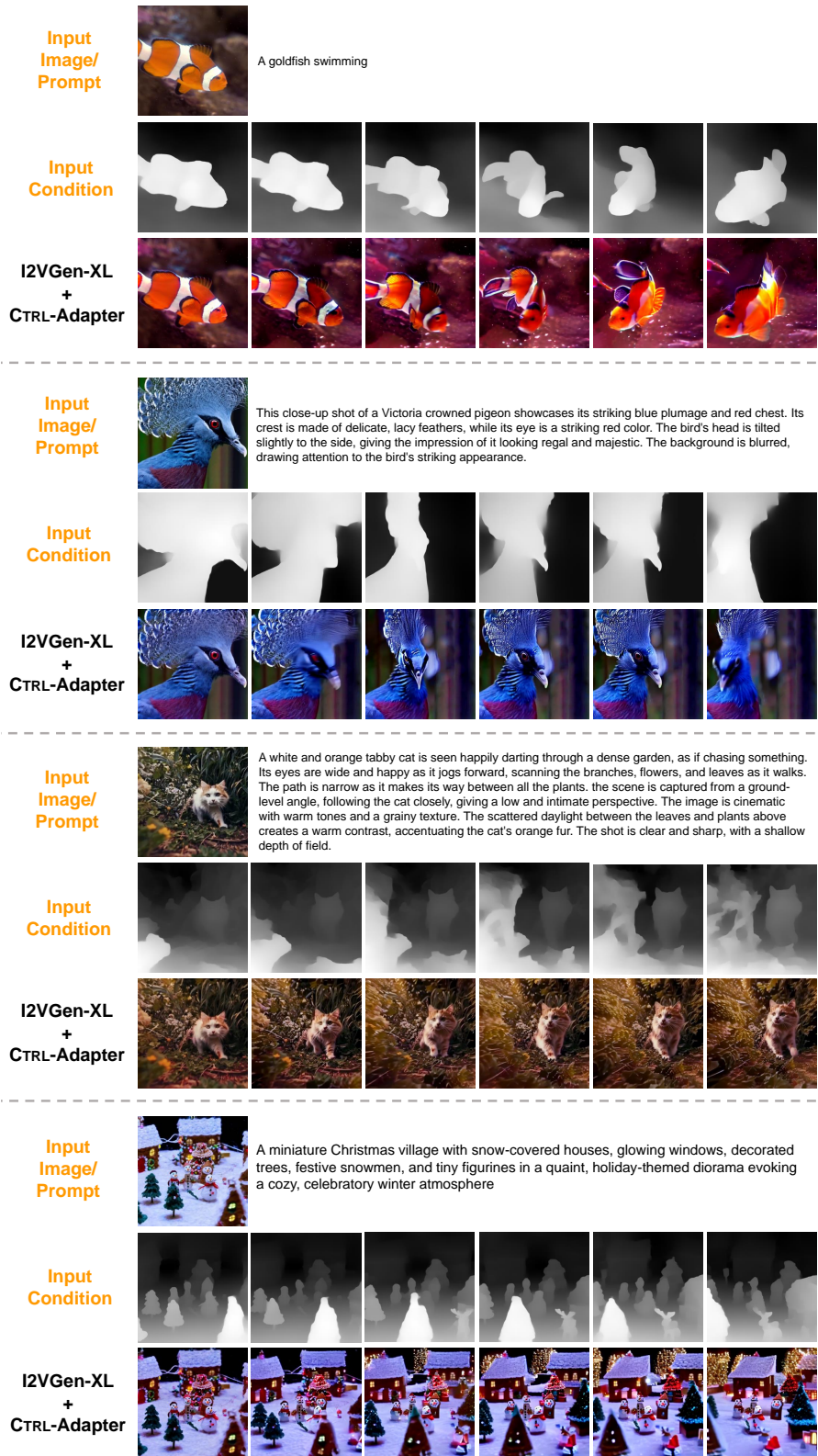


Figure 28: Video generation results with I2VGen-XL using **depth map** as a control condition. See our project page for the full videos.

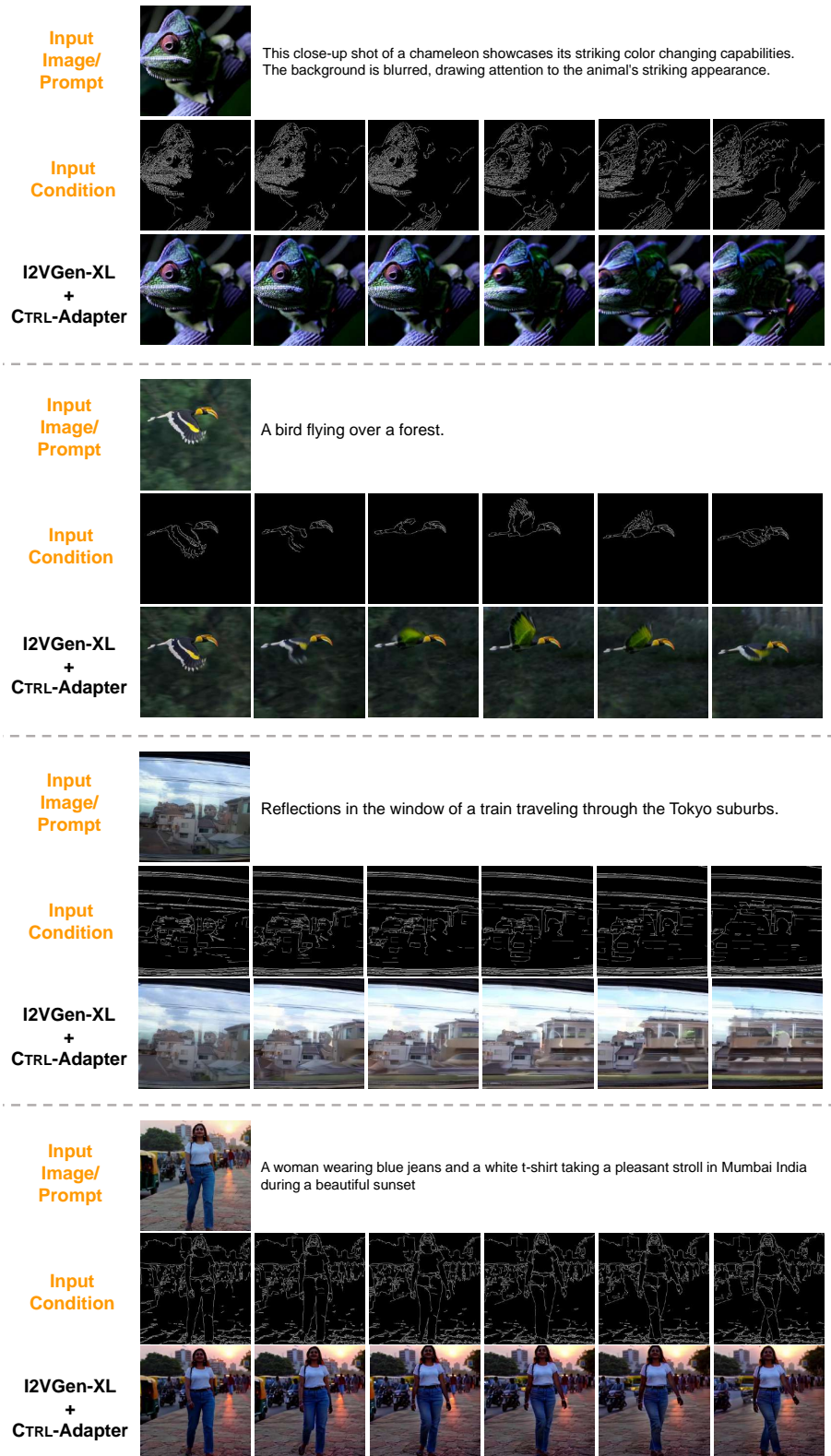


Figure 29: Video generation results with I2VGen-XL using **canny edge** as a control condition. See our project page for the full videos.

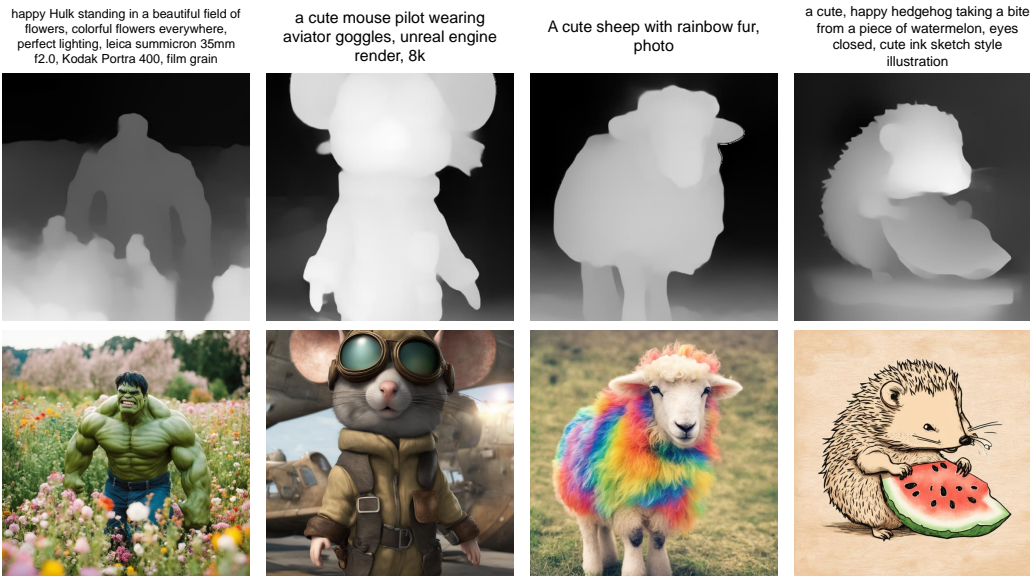


Figure 30: Image generation results from Lexica prompts with SDXL using **depth map** as a control condition.

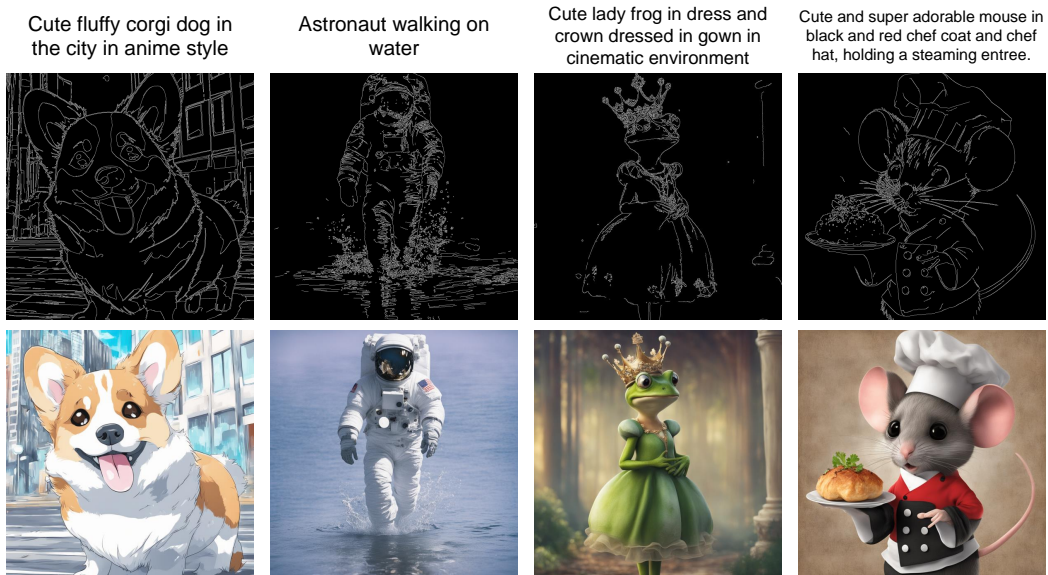


Figure 31: Image generation results from Lexica prompts with SDXL using **canny edge** as a control condition.